

STUDY OF POLYMER FLOW BEHAVIOR IN CAVITY FILLING OF
ALIGNMENT STRUCTURES IN MICRO HOT EMBOSSING

THESIS

Presented to the Graduate Council of
Texas State University-San Marcos
in Partial Fulfillment
of the Requirements

for the Degree

Master of SCIENCE

by

Juan A. Gomez, B.S.

San Marcos, Texas
August 2012

STUDY OF POLYMER FLOW BEHAVIOR IN CAVITY FILLING OF
ALIGNMENT STRUCTURES IN MICRO HOT EMBOSSING

Committee Members Approved:

Byoung Hee You, Chair

Yoo Jae Kim

In-Hyouk Song

Approved:

J. Michael Willoughby
Dean of the Graduate College

COPYRIGHT

by

Juan A. Gomez

2012

FAIR USE AND AUTHOR'S PERMISSION STATEMENT

Fair Use

This work is protected by the Copyright Laws of the United States (Public Law 94-553, section 107). Consistent with fair use as defined in the Copyright Laws, brief quotations from this material are allowed with proper acknowledgment. Use of this material for financial gain without the author's express written permission is not allowed.

Duplication Permission

As the copyright holder of this work I, Juan A. Gomez, authorize duplication of this work, in whole or in part, for educational or scholarly purposes only.

ACKNOWLEDGEMENTS

I especially want to thank my committee chair and advisor, Dr. Byoung Hee You, for all his guidance and support during my research and study at Texas State University-San Marcos. His constant support and motivation guided me through this learning process and encouraged me to never give up when things seemed unfavorable. He once said that in Korea he would be considered as my academic father and he actually became one and I am thankful for that.

It was also a pleasure working with the members of my committee: Dr. Yoo Jae Kim and Dr. In-Hyouk Song who were available and willing to help me during all the research. I also want to thank Dr. Andy Batey for giving me the opportunity of being here and for all the advices he gave me since my first day. I wish to thank the entire faculty, especially the ones I took classes with, for the things I learned these years.

My deepest gratitude goes to my family, my parents: Esperanza Ortega and Guillermo Gomez, and my sister: Maria Angelica Gomez, who always believed and supported me no matter what. All my achievements will always be thanks to them. There is no way I could made it up to here without counting with the support from the people I love the most.

Last but not least, my most sincere gratitude to the Mantilla family, especially Ruth and Fabian Mantilla, for all their kindness and support. I can't imagine how hard this could be without you.

This manuscript was submitted on Tuesday, July 10, 2012

TABLE OF CONTENTS

	Page
ACKNOWLEDGEMENTS	v
LIST OF TABLES	viii
LIST OF FIGURES	ix
ABSTRACT	xiii
CHAPTER 1	1
INTRODUCTION	1
<i>1.1 Motivation</i>	1
<i>1.2 Background</i>	1
<i>1.3 Objective</i>	6
<i>1.4 Outline of the thesis</i>	7
CHAPTER 2	8
NUMERICAL ANALYSIS	8
<i>2.1 Theoretical model</i>	8
<i>2.2 Boundary conditions and limitations</i>	10

2.3	<i>Alignment structure</i>	12
2.4	<i>Simulation model</i>	13
2.5	<i>Material properties</i>	15
2.6	<i>Mesh generation and grid Sensitivity</i>	17
CHAPTER 3		21
DISPLACEMENT CONTROLLED SIMULATIONS		21
3.1	<i>Plane stress simulation</i>	21
3.1.1	<i>Hemisphere-tipped post</i>	21
3.1.2	<i>Hemisphere-tipped post with an annular ring</i>	29
3.2	<i>Chapter conclusion</i>	36
CHAPTER 4		38
FORCE CONTROLLED SIMULATIONS		38
4.1	<i>Simulation conditions</i>	38
4.2	<i>Axisymmetric simulation</i>	40
4.2.1	<i>Hemisphere-tipped post</i>	40
4.2.2	<i>Hemisphere-tipped post with an annular ring</i>	48
4.3	<i>Conclusions</i>	60
CHAPTER 5		62
CONCLUSIONS		62
REFERENCES		66

LIST OF TABLES

Table	Page
Table 1. Coefficients for the molding temperatures	9
Table 2. Material properties of the polymer and mold [Yao et al., 2005]	15
Table 3. Flow stress used in embossing calculation at a strain rate of 0.0001	16

LIST OF FIGURES

Figure	Page
Figure 1. Schematic representation of hot the embossing process	10
Figure 2. Two boundary conditions included in the numerical analysis: (a) Plane stress boundary condition and (b) Axisymmetric boundary condition.....	11
Figure 3. Alignment structures used in the numerical analysis of flow behavior in cavity filling: (a) hemisphere-tipped post and (b) hemisphere-tipped post with an annular ring.13	13
Figure 4. Flow Stress of PMMA at a strain rate of 0.0001	17
Figure 5. Grid Sensitivity analyses in (a) Plane stress simulation and Axisymmetric simulation.....	18
Figure 6. FEM model for the analysis of flow behavior of polymer during mold filling: (a) hemisphere-tipped post and (b) hemisphere-tipped post with an annular ring	19
Figure 7. Stress evolution of a molded hemisphere-tipped post at the bottom edge of the mold and the flow front of polymer with a molding temperature of 87.5°C.....	22
Figure 8. Stress distribution of a molded hemisphere-tipped post in mold filling while the displacement increase from 1.0 mm to 2.5 mm: (a) Mold displacement of 1.0 mm, (b) Mold displacement of 1.5 mm, (c) Mold displacement of 2.0mm, and (d) Mold displacement of 2.5mm.....	23
Figure 9. Stress evolution of a molded hemisphere-tipped post at the bottom edge of the mold and the flow front of polymer with a molding temperature of 112.5°C.....	24
Figure 10. Stress distribution of a molded hemisphere-tipped post in mold filling while the displacement increase from 1.0 mm to 2.5 mm: (a) Mold displacement of 1.0 mm and (d) Mold displacement of 2.5 mm.....	25
Figure 11. Stress evolution of a molded hemisphere-tipped post at the bottom edge of the mold and the flow front of polymer with a molding temperature of 150°C.....	26
Figure 12. Stress distribution of a molded hemisphere-tipped post in mold filling while the displacement increase from 1.0 mm to 2.5 mm: (a) Mold displacement of 1.0 mm and (b) Mold displacement of 1.5 mm.....	27

Figure 13. Heights of the molded posts at the molding temperatures of 87.5, 112.5, and 150°C when the displacement increased from 0.5 mm to 2.5 mm.	28
Figure 14. Stress evolution of a molded hemisphere-tipped post with an annular ring at the bottom edge of the mold and the flow front of polymer with a molding temperature of 87.5°C	29
Figure 15. Stress distribution of a molded hemisphere-tipped post with an annular ring in mold filling while the displacement increase from 1.0 mm to 2.5 mm: (a) Mold displacement of 1.0 mm, (b) Mold displacement of 1.5 mm, (c) Mold displacement of 2.0mm, and (d) Mold displacement of 2.5 mm.....	30
Figure 16. Stress evolution of a molded hemisphere-tipped post with an annular ring at the bottom edge of the mold and the flow front of polymer with a molding temperature of 112.5°C	31
Figure 17. Stress distribution of a molded hemisphere-tipped post with an annular ring in mold filling while the displacement increase from 1.0 mm to 2.5 mm: (a) Mold displacement of 1.0 mm, (b) Mold displacement of 1.5 mm,.....	32
Figure 18. Stress evolution of a molded hemisphere-tipped post with an annular ring at the bottom edge of the mold and the flow front of polymer with a molding temperature of 150°C	33
Figure 19. Stress distribution of a molded hemisphere-tipped post with an annular ring in mold filling while the displacement increase from 1.0 mm to 2.5 mm: (a) Mold displacement of 1.0 mm, (b) Mold displacement of 1.5 mm, and (c) Mold displacement of 2.0 mm	35
Figure 20. Heights of the molded posts at the molding temperatures of 87.5, 112.5, and 150°C when the displacement increased from 0.5 mm to 2.5 mm.	36
Figure 21. Application of the load depending on molding time	39
Figure 22. Force controlled matrix at T1 = 87.5°C, T2 = 112.5, and T3 = 150°C	39
Figure 23. Stress evolution of a molded hemisphere-tipped post at the bottom edge of the mold and the flow front of polymer with a molding temperature of 150°C and a molding force of 300 N	40
Figure 24. Stress distribution of a molded hemisphere-tipped post in mold filling while the displacement increase from 1.0 mm to 2.5 mm: (a) Mold displacement of 1.0 mm, (b) Mold displacement of 1.5 mm, (c) Mold displacement of 2.0mm, and (d) Mold displacement of 2.5 mm.....	42

Figure 25. Stress evolution of a molded hemisphere-tipped post at the bottom edge of the mold and the flow front of polymer with a molding temperature of 150°C and a molding force of 600 N	43
Figure 26. Stress distribution of a molded hemisphere-tipped post in mold filling while the displacement increase from 1.0 mm to 2.5 mm: (a) Mold displacement of 1.0 mm, (b) Mold displacement of 1.5 mm, (c) Mold displacement of 2.0 mm, and (d) Mold displacement of 2.5 mm	44
Figure 27. Stress evolution of a molded hemisphere-tipped post at the bottom edge of the mold and the flow front of polymer with a molding temperature of 150°C and a molding force of 900 N	45
Figure 28. Stress distribution of a molded hemisphere-tipped post in mold filling while the displacement increase from 1.0 mm to 2.5 mm: (a) Mold displacement of 1.0 mm, (b) Mold displacement of 1.5 mm, (c) Mold displacement of 2.0mm, and (d) Mold displacement of 2.5 mm	46
Figure 29. Heights of the molded posts at the molding temperatures of 87.5, 112.5, and 150°C when the displacement increased from 0.5 mm to 2.5 mm.	47
Figure 30. Stress evolution of a molded hemisphere-tipped post with an annular ring at the bottom edge of the mold and the flow front of polymer with a molding temperature of 112.5°C and a molding force of 300 N	48
Figure 31. Stress distribution of a molded hemisphere-tipped post in mold filling while the displacement increase from 0.25 mm to 0.50 mm: (a) Mold displacement of 0.25 mm and (b) Mold displacement of 0.5 mm	49
Figure 32. Stress evolution of a molded hemisphere-tipped post with an annular ring at the bottom edge of the mold and the flow front of polymer with a molding temperature of 150°C and a molding force of 300 N	50
Figure 33. Stress distribution of a molded hemisphere-tipped post in mold filling while the displacement increase from 1.0 mm to 2.5 mm: (a) Mold displacement of 1.0 mm, (b) Mold displacement of 1.5 mm, (c) Mold displacement of 2.0mm, and (d) Mold displacement of 2.5 mm	51
Figure 34. Stress evolution of a molded hemisphere-tipped post with an annular ring at the bottom edge of the mold and the flow front of polymer with a molding temperature of 112.5°C and a molding force of 600 N	52
Figure 35. Stress distribution of a molded hemisphere-tipped post in mold filling while the displacement increase from 0.25 mm to 0.50 mm: (a) Mold displacement of 0.25 mm and (b) Mold displacement of 0.50 mm	53

Figure 36. Stress distribution of a molded hemisphere-tipped post in mold filling while the displacement increase from 1.0 mm to 2.5 mm: (a) Mold displacement of 1.0 mm, (b) Mold displacement of 1.5 mm, (c) Mold displacement of 2.0mm, and (d) Mold displacement of 2.5 mm..... 55

Figure 37. Stress evolution of a molded hemisphere-tipped post with an annular ring at the bottom edge of the mold and the flow front of polymer with a molding temperature of 112.5°C and a molding force of 900 N..... 56

Figure 38. Stress distribution of a molded hemisphere-tipped post in mold filling while the displacement increase from 0.25 mm to 0.50 mm: (a) Mold displacement of 0.25 mm and (b) Mold displacement of 0.50 mm..... 57

Figure 39. Stress evolution of a molded hemisphere-tipped post with an annular ring at the bottom edge of the mold and the flow front of polymer with a molding temperature of 150°C and a molding force of 900 N..... 58

Figure 40. Stress distribution of a molded hemisphere-tipped post in mold filling while the displacement increase from 1.0 mm to 2.5 mm: (a) Mold displacement of 1.0 mm, (b) Mold displacement of 1.5 mm, (c) Mold displacement of 2.0mm, and (d) Mold displacement of 2.5 mm..... 59

Figure 41. Heights of the molded posts at the molding temperatures of 87.5, 112.5, and 150°C when the displacement increased from 0.5 mm to 2.5 mm.60

ABSTRACT

STUDY OF POLYMER FLOW BEHAVIOR IN CAVITY FILLING OF ALIGNMENT STRUCTURES IN MICRO HOT EMBOSSING

by

Juan A Gomez, B.S.

Texas State University-San Marcos

August 2012

SUPERVISING PROFESSOR: BYOUNG HEE YOU

The behavior of polymer flow is a critical aspect in micro hot embossing. The flow behavior significantly depends on the process parameters including molding temperatures and displacement of a mold with respect to a polymer substrate. To achieve accurate replication of microstructures, it is necessary to predict the flow behavior depending on the process parameters.

Two alignment structures were chosen as embossing features to demonstrate the flow behavior of polymer in hot embossing. The post has a height of 925 μm and a radius of 500 μm . Polymethyl-Methacrylate (PMMA) was selected as a substrate material. Computer-aided engineering models (CAE), using DEFORM 2D (SFTC, Columbus, OH), were used to simulate the flow behavior in the filling of a hemisphere-tipped cavity

in molding. Simulations were performed to help understand the flow behavior of the polymer while varying the molding temperatures and the displacement of the mold. The simulation conditions were mold temperatures of 75, 100, 125, and 150°C, displacement of mold of 0.5, 1.0, 2.0, 2.5 mm, and speed of embossing 0.008 mm/sec.

Replication fidelity of the post was evaluated using the height of molded hemisphere-tipped post. The height of the molded post increases while the molding temperature and displacement increase. Incomplete filling of polymer at the cavity was observed at molding temperature of 75°C when the displacement increased from 0.5 mm to 2.5 mm. As molding temperature increased to 125°C, the cavity was completely filled at the displacement of 1.5, 2.0, and 2.5 mm. The increase of mold temperature yielded better cavity filling because the higher molding temperature decreased the fluidic resistance of the polymer. It can be explained by a glass transition temperature of PMMA, about 105°C, so PMMA significantly softens above this temperature.

Numerical simulation predicted the flow behavior of polymer in micro hot embossing of the alignment structure. These results can be used to determine proper process parameters for the microfabrication of polymer microstructures.

CHAPTER 1

INTRODUCTION

1.1 Motivation

The flow behaviors of polymers have been considered as a critical aspect for the replication of polymer microstructures in hot embossing [Chen et al., 2007]. The process parameters, including molding temperatures, applied molding forces, and displacements of the die, directly affect the flow behavior to fill a mold cavity during molding [G'sell, 1997] [Worgull, 2003] [Li et al., 2007] [Peng et al., 2009]. Understanding the flow behavior can benefit the molding by designing the proper process parameters. The effects of process parameters can be analyzed in design and manufacturing process. The process parameters can be controlled to achieve high quality of replication. This may lead to a reliable replication of polymer microstructures [Li et al., 2008].

1.2 Background

Hot embossing is a manufacturing technology to transfer features from a mold into polymers. It has been widely used to fabricate polymer microstructures [Heckele and Schomburg, 2004]. Simplicity of a mold change, flexibility of manufacturing for different polymers, high quality of replication, and low temperature cycle of polymer are typical advantages of hot embossing. It is well suited to small and medium-volume production [Luo et al., 2006].

Hot embossing can be divided into three process steps including embossing, cooling, and demolding. Designed features are transferred from the mold into the polymer, while the mold presses the polymer with the embossing force. High molding temperature above the glass transition temperature (T_g) of the polymer is recommended to reduce the fluidic resistance. It promotes the advance of flow front of the polymers to fill the mold cavities [Yao et al., 2005] [He et al., 2007]. The mold and the polymer are cooled down below T_g during cooling. The polymer has larger shrinkage than the shrinkage of the mold. This induces thermal stress at the interfacial layers of the polymers and mold [Jin et al., 2009]. The polymers are separated from the mold in demolding. The replicated features can be damaged due to the demolding force, so minimizing the demolding force is also one of the critical aspects to produce reliable polymer microstructures [Song et al., 2008].

The molding temperature, die displacement, embossing force, and demolding force are principal process parameters in hot embossing. The cavity filling with polymers is a foundation stone for the replication of the features. Analysis of flow behavior can provide design information to ensure mold filling. Various analyses have been performed to select the proper process parameters for mold filling [Yao et al., 2005] [He et al., 2007].

A theoretical model was introduced to compute a required embossing time to fill a micro square cavity with polymers [Heyderman et al., 2000]. The analysis was based on a simple two-dimensional squeeze flow theory of polymers and it reflected a hydrostatic pressure applied on the polymer in the computation. The model was not expanded to the mold filling with complicated mold geometrics.

Juang studied the flow behaviors of polymers for both isothermal and non-isothermal embossing using a commercial finite element simulation code, DEFORM-2D (Scientific Forming Technologies Corp., Columbus, Ohio) [Juang et al., 2002]. The predicted flow patterns of isothermal embossing agreed with the experimental results but simulations did not consider the effect of backup pressure on the polymer due to an air entrapment because the software was not able to simulate the phenomena. A weld line appeared in non-isothermal embossing due to the collision of two molten and solidified layers.

Numerical analyses of non-isothermal embossing were performed by Yao. A commercial finite simulation code, MARC (MSC Software Co.) was used to compute the mold filling [Yao, et al., 2005]. The advance of the flow front polymers was correlated with the ratio of heat transfer from a mold cavity to polymers, while the depths of cavities varied from 200 μm to 0.5 μm . The results of simulations reported uniform or non-uniform flow patterns of polymers depending on the different depths of the microcavities.

Experimental and simulation methods were used to analyze the flow patterns of PMMA in isothermal hot embossing [Kim et al., 2004] the numerical analyses showed the effect of the number of cavities, the distance between the cavities, and a surface tension of PMMA. Experimental testing consisted of isothermal hot embossing at 130°C and constant values of pressure and vacuum. Embossing times of 10s, 20s, 30s, 1min, 2min, 3min, and 5min were used to observe filling patterns and capillary effects. Typical flow characteristics were perceived. At the first moment, polymer flows in the upward direction along the wall of the cavity. The numerical analysis was done using a commercial Computational Fluid Dynamics (CFD) code Flow-3D [Flow Science, Inc.,

Leland, North Carolina). Using plane strain simulations with cavity ratios of depth and width between 0.5 and 200, embossing time of 6 min, and temperatures between 190 and 230°C were included in the analysis. In the analyses, polymers flowed up along the side wall first, followed by the center in the mod cavity. The predicted flow behavior was verified by showing the advance of flow front.

Young (2005) developed a tool to predict polymer flow behavior based on a viscous model using Polystyrene (PS) as polymer substrate. The first approach included a single-feature embossing process. The dimensions of the feature were: 100 nm width and 500 nm height. Isothermal embossing was simulated at 160 and 180°C. Results demonstrated that flow behavior was relatively similar to the experimental observations made by Juang et al. (2002). A second study was developed to analyze polymer flow and cavity filling behavior in multi-feature imprint patterns. Feature distances varied from 200 to 900 nm. High-pressure points were located around the imprint feature. While the mold is beginning to compress the polymer an important increase in pressure was observed due to the occurrence of large polymer flow on the planar direction. As it was expected, the embossing pressure is higher at lower temperatures. Filling capacity of the polymer will depend on the cavity thickness and height.

Luo studied the effect of embossing time on the viscoelastic behavior of PMMA during mold filling [Luo et al., 2006]. The time dependence of a strain of PMMA was obtained from creep experiment and it was coupled with numerical models using third order polynomial and first order exponential decay formulae. The results of this study demonstrated that the first order exponential decay was a more accurate model to predict the flow behavior of the polymer.

Isothermal hot embossing was analyzed to estimate the heights of mold filling with concave and convex features. The simulation was performed using DEFORM-2D to show mold filling with PMMA [He et al., 2007]. The heights were evaluated with the movement of the flow fronts of PMMA as functions of embossing time and the location of features from a center of the mold.

A simulation method was proposed to characterize the flow behavior and recovery of polymer [Jin et al, 2009]. Polymer was regarded as a non-Newtonian fluid during mold filling and a linear-elastic solid after demolding. The proposed model allowed the simulation to predict the recovery of the polymers after demolding. The recovery of polymer, obtained from the simulations, was in a good agreement with the experimental results [Jin et al, 2009] [Zhang et al., 2011].

The stress evolution of polymers was analyzed for an isothermal hot embossing, while the mold had various mold geometries including a duty ratio, aspect ratio, width to thickness ratios, and cavity location [Zhang et al, 2011]. A stress barrier was proposed to reduce the defects of replicated structures. The small duty ratio and high aspect ratio of the mold cavity significantly contribute to the stress concentration developed at the bottom edge of the replicated structure.

The effects on stamp geometry, shear thinning and imprint speed of a viscous polymer was studied by Jing et al. (2009). They simulated a three-stage hot embossing process using DEFORM 2D Computer Aided Engineering (CAE) software. Results showed that deformation depends on the ratio cavity width to height, the ratio cavity width to tool width and the temperature influence of imprint speed. The deformation

follows different polymer deformation modes (single and dual peaks and then an embossing stage).

Mold filling analysis has significance for the replication polymer microstructures in hot embossing. The flow behavior can be analyzed as a function of the process parameters and stress evolution on the polymer to the reliable replication.

1.3 Objective

The objective of this research is to gain better understanding of the flow behavior of polymers for the reliable replication of two alignment structures for assembly of microdevices. Two alignment structures, a hemisphere-tipped post and a hemisphere-tipped post with an annular ring, were chosen as a demonstration of the numerical analyses. Two-dimensional computer-aided engineering (CAE) models, using DEFORM-2D, is used to characterize the flow behavior during mold filling. The heights of model filling with polymer were evaluated as a function of process parameters, including molding temperatures, displacements of dies, and embossing forces.

The goals of this research are:

- a. Understand of polymer flow behavior depending on the pattern
 - Case 1: the flow behavior in the hemisphere-tipped hole
 - Case 2: the flow behavior in the hemisphere-tipped holes with annual ring
- b. Develop the foundation and initial approach for a design tool using simulation for the replication of reliable polymer microstructures

1.4 Outline of the thesis

The theoretical model, boundary conditions, material properties, the simulation model, and the numerical analyses of mold filling to investigate the flow behavior of polymer are covered in the following chapters.

Chapter 2 includes governing equations, boundary conditions, assumptions, and limitations for numerical analysis. This chapter also contains the material models of PMMA, grid sensitivity, and the power-law model used to define the temperature dependence of the polymer.

Simulations were performed using displacement control of a die in Chapter 3. Molding temperatures, the movement of the die, and size of edges were considered in the analysis.

Chapter 4 represents force controlled simulations. Results are analyzed the effect of applied molding forces on the replication fidelity, depending on the molding temperatures and a radius of the edges.

Conclusions and recommendations can be found on chapter 5.

CHAPTER 2

NUMERICAL ANALYSIS

A finite element analysis software, DEFORM 2D (Scientific Forming Technologies, OH) was used to analyze the flow behavior of polymers during mold filling. DEFORM 2D is a commercial code designed to simulate two-dimensional flow of metal forming processes including forging, rolling, and extrusion. It has been widely used in the simulation of the flow behavior of polymer for the molding of hot embossing. [Juang et al., 2002] [Yao et al., 2005] [He et al., 2007] [Jing et al., 2009].

This chapter includes the governing equations, assumptions and limitations of the theoretical models, boundary conditions, defined geometries, and the simulation models for the numerical analyses.

2.1 Theoretical model

The governing equations defined in this chapter are used as an introductory approach to viscoelasticity analysis.

Mass conservation equation:

$$v_{i,j} = 0, \quad (1)$$

where, v_i is a velocity component, “,” expresses the differentiation and i,j are the components. [Yao et al, 2005]

Force balance equilibrium equation:

$$\sigma_{ij,j} = 0, \quad (2)$$

where σ_{ij} is a stress component in the $-X, -Y$ plane. [Yao et al, 2005]

Strain rate-velocity relation:

$$\varepsilon_{ij} = \frac{1}{2}(v_{i,j} + v_{j,i}) \quad (3)$$

where ε_{ij} is the strain rate component and $v_{i,j} + v_{j,i}$ are the velocity components.

Energy conservation equation:

$$\rho C_p T = k T_{i,j} + \sigma_{ij} \varepsilon_{ij} \quad (4)$$

where ρ is the density, C_p is the heat capacity of the material, k the thermal conductivity, and T is the temperature. The stress and strain components on the equation are referring to the modulus of elasticity of the polymer substrate.

Flow stress and polymer behavior can be defined using the relationship between stress and strain under constant strain rates. The relation is expressed on equation 5.

[Juang et al., 2002]

$$\sigma = c \dot{\varepsilon}^k \quad (5)$$

where σ is the flow stress [MPa], $\dot{\varepsilon}$ is the strain rate [He et al, 2007] and c and k are coefficients for the molding temperatures. Table 1 show the coefficients used in the numerical analysis. Coefficients for the molding temperatures were obtained by calculating the trend of the behavior observed by Juang (2002).

Table 1. Coefficients for the molding temperatures

		25°C	95°C	100°C	140°C	250°C
Strain Rate ($\varepsilon = 0.0001$)	c	76.021	37.724	5.5	0.06	0.006
	k	0.0233	0.1374	2×10^{-16}	-2×10^{-16}	0
Strain Rate ($\varepsilon = 1$)	c	79.027	41.089	5.5	1.16	0.006
	k	0.00224	0.1287	2×10^{-16}	0.32	0

Material data was fitted for log interpolation using the power law model. Flow stress values are interpolated based on log strain, log strain rate and temperature [Scientific Forming Technologies Corporation (SFTC), 2010]. Equation 6 shows the power law model used for log interpolation.

$$\sigma = c\epsilon^{-n}\dot{\epsilon}^{-m} + y \quad (6)$$

where σ is the flow stress [MPa], ϵ is a strain, c is the material constant, y is the initial yield value and n and m are strain and strain rate exponents respectively calculated by the simulation software.

The polymer was considered as a viscoelastic fluid above its glass transition temperature [Zhang et al., 2011]. Friction between the mold and the polymer substrate was not considered in the analysis to reduce calculation time [Young et al., 2005]. Both top and bottom dies were defined as rigid bodies. The polymer substrate was assumed as a deformable body. Isothermal embossing was analyzed.

2.2 Boundary conditions and limitations

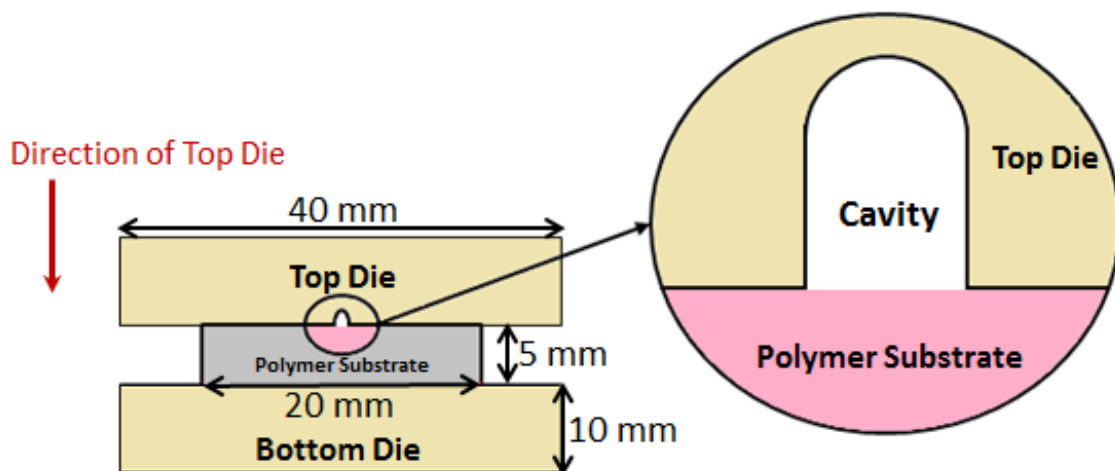


Figure 1. Schematic representation of hot the embossing process.

The schematic representation of hot embossing process performed in this study is shown in Figure 1. A polymer substrate was located between the top and bottom dies. Both dies had a width of 40 mm and a thickness of 10 mm. The top die contained a feature on the mold for a hemisphere-tipped hole. The substrate was 20mm, with a thickness of 5mm.

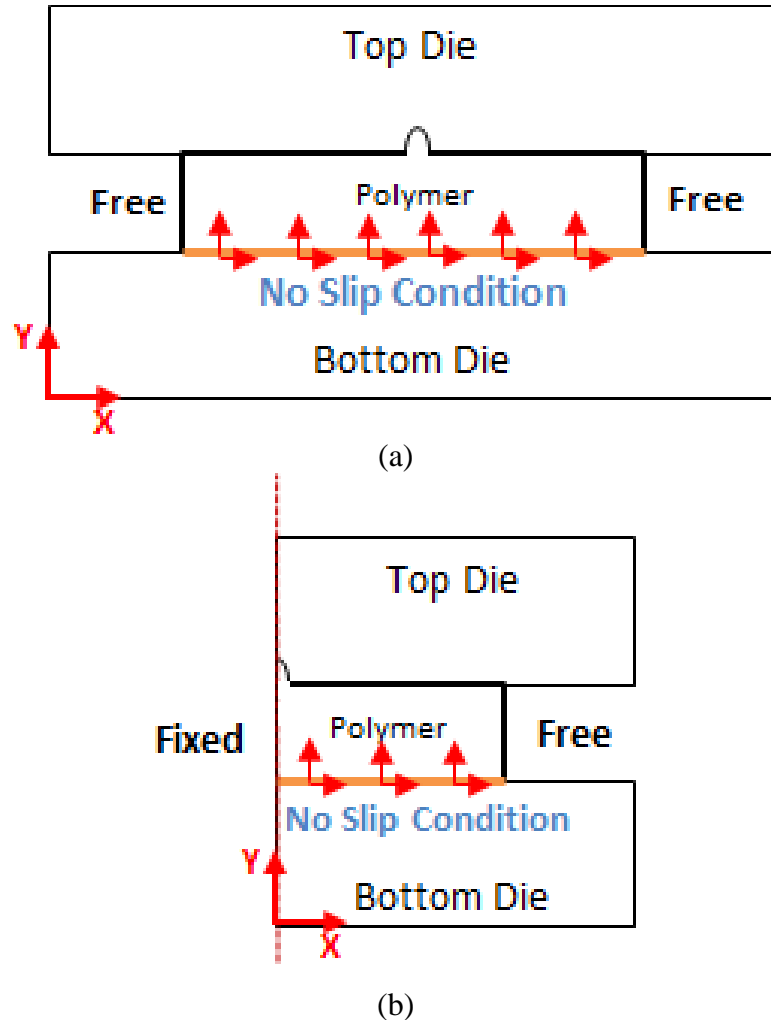


Figure 2. Two boundary conditions included in the numerical analysis: (a) Plane stress boundary condition and (b) Axisymmetric boundary condition.

The hemisphere-tipped hole was located at the center of the top die. Movement direction of the top die is indicated by the arrows located above it. The displacement will apply pressure on the surface of the material substrate forcing it to flow into the

hemisphere-tipped hole. Polymethyl-Methacrylate (PMMA) was selected as the polymer substrate for the replication of alignment structures. The enlarged area shows the contact area between the hemisphere-tipped hole and the polymer substrate.

Plane stress and axisymmetric boundary conditions for the numerical analyses were considered as shown in Figure 2. The plane stress model assumed that the polymer flows identically in any cross-sectional area on the X- and Y- plane as shown in Figure 2(a). The finite element code considers a depth of one unit across the section. A unit depth of 1 mm was adopted in the numerical analysis. Figure 2(b) illustrates the axisymmetric boundary conditions. The axisymmetric model postulates that the geometry is symmetric along the center axis of the X- and Y- plane. The degrees of freedom preceding the X- and Y- plane, on the center line was fixed. X- and Y- degrees of freedom were also constrained on the bottom surface of the substrate by using a sticking condition. No constraint was applied at the edges of the polymer substrate.

Contact was generated by means of an inter-object relationship in the simulation. The inter-object relation defines what and how contacting objects are supposed to behave while in contact. The behavior is assigned by the master-slave combination. The master-slave consolidate illustrates that deforming objects should be considered as slaves always. The top die was defined as the master object and the polymer substrate was considered as the slave object. Constant speed was adapted to the mold. The movement of the top die was controlled using an assigned displacement or force on the die.

2.3 Alignment structure

Two alignment structures for assembly of microfluidic devices were selected to demonstrate the flow behavior of polymer in hot embossing. Figure 3 illustrates the

dimensions and geometry of both alignment structures including a hemisphere-tipped post and a hemisphere-tipped post with an annular ring. The hemisphere-tipped post is a basic alignment structure with a post height of $925\ \mu\text{m}$, a radius of $500\ \mu\text{m}$, and a cavity thickness of $1\ \text{mm}$ as shown in Figure 3(a).

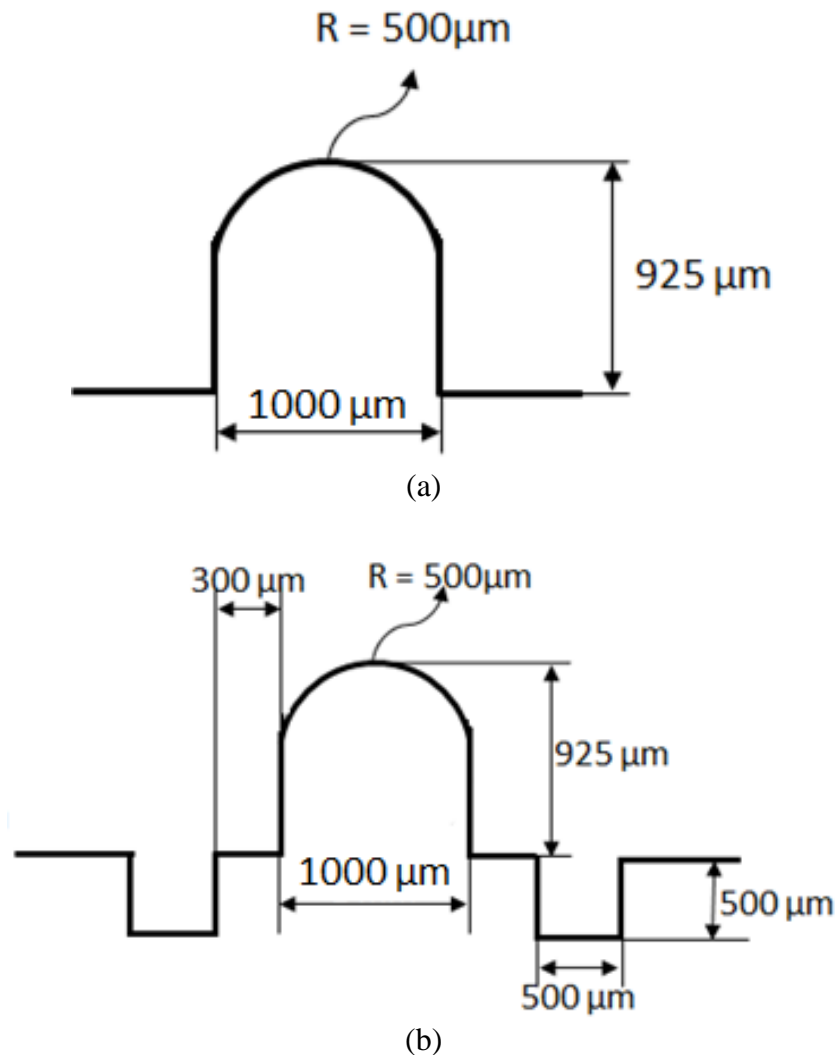


Figure 3. Alignment structures used in the numerical analysis of flow behavior in cavity filling: (a) hemisphere-tipped post and (b) hemisphere-tipped post with an annular ring.

An annular structure added around the hemisphere-tipped post was proposed as an approach to promote the polymer flow phenomena and reduce the deformation effect in embossing. Figure 3(b) represents the hemisphere-tipped post with an annular ring. The

cavity had the same height, radius, and thickness dimensions as the hemisphere-tipped post. The annular structure was separated 300 μm from the hemisphere-tipped post. The annular ring had a height of 500 μm and a thickness of 500 μm .

2.4 Simulation model

Simulations were divided into two geometric models including axisymmetric and plane stress models. The geometric models can be accessed in the simulation controls window on the pre-processor of the finite element code. The simulation was configured in the deformation-only mode. The deformation-only mode did not consider heat transfer between objects. Mold displacement was applied by a displacement of the top die and applied force on the top die. Displacement controlled simulations consider that the mold must achieve a total specified movement. Total displacements of 0.5, 1.0, 1.5, 2.0, and 2.5 mm were used with a fixed continuous speed of 0.0084 mm/sec. force controlled simulations apply a load on the surface of the polymer substrate during a specified period of time or until the mold completes the expected displacement. The forces of 300, 600, and 900 N were applied.

The effect that the shape of the mold causes on the polymer substrate was studied by the addition of a small radius of one-twentieth of the cavity thickness on the edge of the mold.

To analyze the effect that the embossing temperature generates on the behavior of polymers during cavity filling, molding temperatures of 75, 87.5, 100, 112.5, 125, 137.5, and 150 $^{\circ}\text{C}$ were included in the numerical analysis to have better understanding of the polymer behavior at the different material stages.

Computation steps can be controlled by time or by the displacement of the mold. Displacement controlled simulations are based on a step definition of die displacement. The step definition of displacement controlled simulations will allow the master object to move only a reduced limited distance per step. Force controlled simulations use a step definition of time increment meaning that the total simulation time is divided by the number of steps. The step definition number is calculated by the size of the smallest element divided by ten. The step definition was established as 0.001 mm/step for displacement controlled simulations and 0.001 sec/step for force controlled simulations.

The total number of steps can be calculated using Equation 7 [SFTC, 2010].

$$n = \frac{x}{V\Delta t} \quad (7)$$

where, x is the total movement of the master object, V is the velocity of the primary die and Δt is the time increment per step.

2.5 Material properties

Material properties of the polymer substrate and both the top die and the bottom die are included in Table 1. PMMA was chosen as a substrate material because of its popularity and its acceptable properties, relatively low cost and easy handling and processing. It has a density of $1.17 \times 10^3 \text{ kg/m}^3$, a thermal conductivity of 0.2 W/mk , and a specific heat of 1500 J/Kg-k . [Yao et al., 2005]

Table 2. Material properties of the polymer and mold [Yao et al., 2005]

	Material	Density (Kg/m ³)	Thermal Conductivity (W/(m·K))	Specific Heat (J/Kg-K)	Young's Modulus (GPa)
Polymer	PMMA	1.17×10^3	0.2	1500	3.1
Die	Brass alloy 360	8940	115	445	97.0

The material selected for both top die and bottom die was Brass alloy 360. It is an alloy of copper and zinc used principally in applications where low friction is required. The density of this alloy is 8940 kg/m^3 , has a thermal conductivity of 115 W/mk , a specific heat of 445 J/Kg-k , and a Young's modulus of 97.0 GPa . [Yao et al., 2005]

Table 3. Flow stress used in embossing calculation at a strain rate of 0.0001

25°C		95°C		100°C		140°C		250°C	
Stress	Strain								
0	0	0	0	0	0	0	0	0	0
75	0.05	31	0.05	5.5	0.05	1.16	0.05	0.006	0.05
73	0.5	24	0.5	5.5	0.5	1.16	0.5	0.006	0.5
83	1	58	1	5.5	1	1.16	1	0.006	1

Stress-Strain relationship of the polymer can define the flow behavior during mold filling with the polymer. Table 2 shows the stress-strain relationship for PMMA, while the molding temperature varies from 25°C to 250°C and a strain rate is fixed at 0.0001. It is obtained from the previous studies by Juang and G'Sell [Yao et al., 2005]. The stress decrease rapidly as the temperature increased.

The stress-strain relationship in Table 1 was coupled to the material properties of PMMA and the power law model was applied to interpolate by the power law model shown in equation 6. Strains were 0, 0.05, 0.5, and 1 mm/mm. the flow stress decreased from 83 MPa to 0.006 MPa as the temperature of the polymer increased from 25°C to 250°C as illustrated in Figure 4. This implies that high molding temperature can reduce significantly the fluid resistance of the polymer in molding.

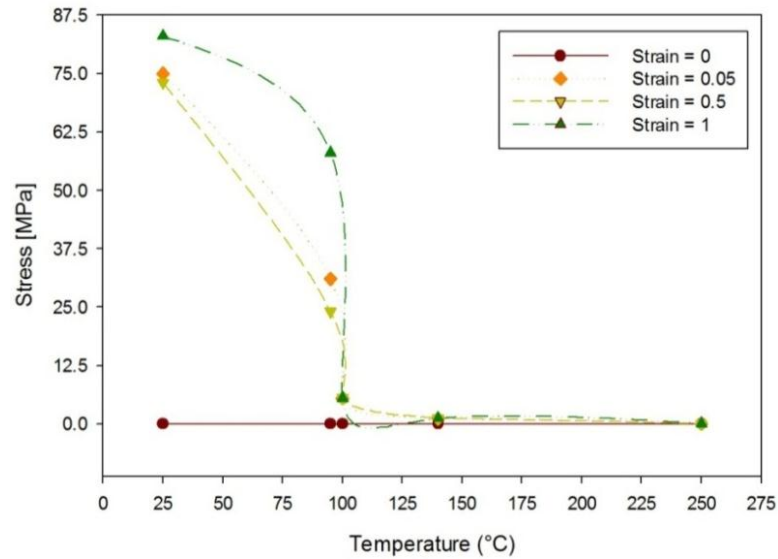
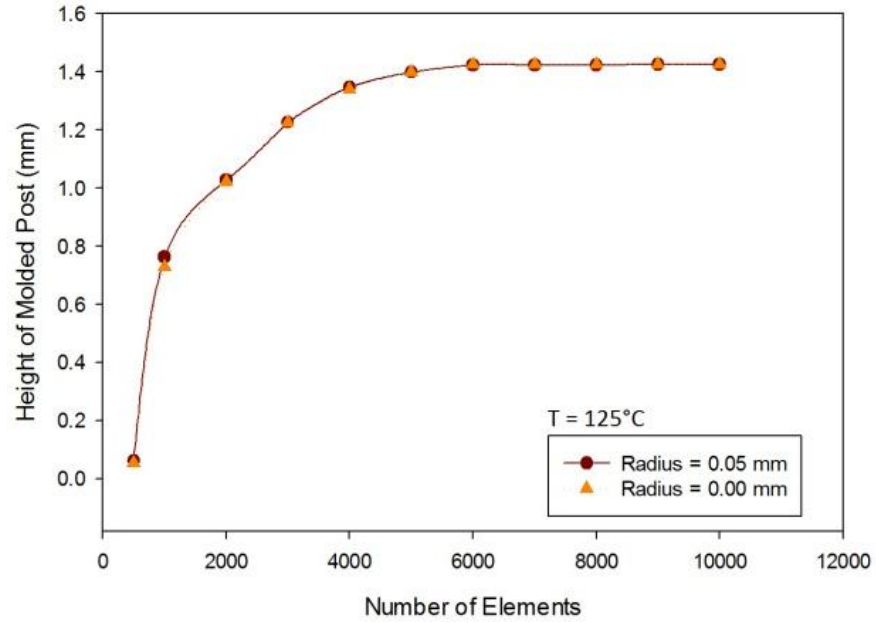


Figure 4. Flow Stress of PMMA at a strain rate of 0.0001.

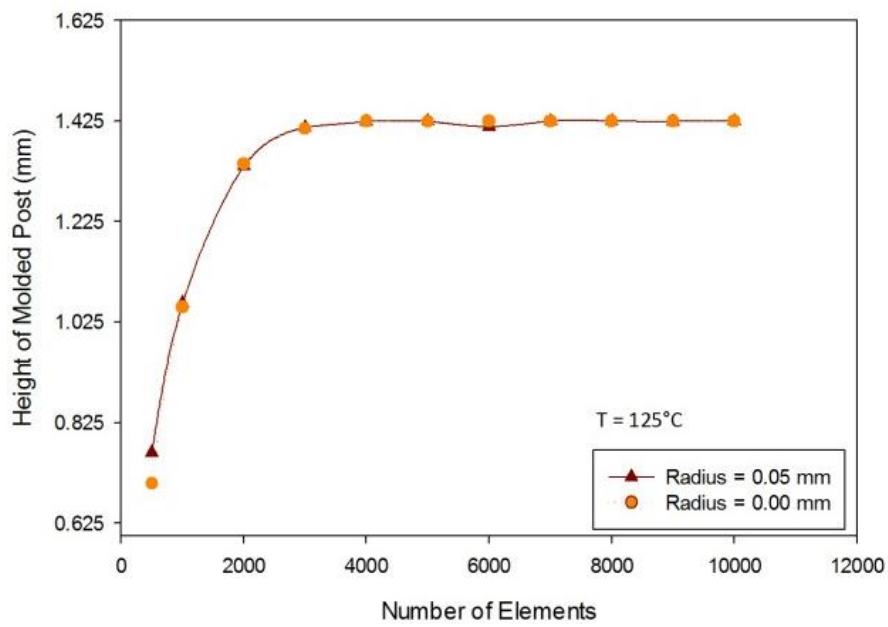
2.6 Mesh generation and grid Sensitivity

Polymer mesh was generated using the mesh generation window inside the pre-processor. The mesh generation windows let the user define the type and density for the mesh needed in certain object. User-Defined mesh was chosen in this study. User-Defined meshing will allow the object to have higher density elements at certain areas of the object compared to other areas, depending on simulation conditions. This approach is used to improve simulation performance without reducing accuracy. Mesh density refers to the size of the elements that will be generated in a defined object. Using the mesh window function various density elements were defined on the model.

Figure 5 shows the number of elements used in the grid sensitivity analysis. Figure 5(a) illustrates plane stress simulation. The height of the molded post reaches equilibrium at 5000 elements. Figure 5(b) shows the grid sensitivity for axisymmetric simulation.



(a)



(b)

Figure 5. Grid Sensitivity analyses in (a) Plane stress simulation and (b) Axisymmetric simulation.

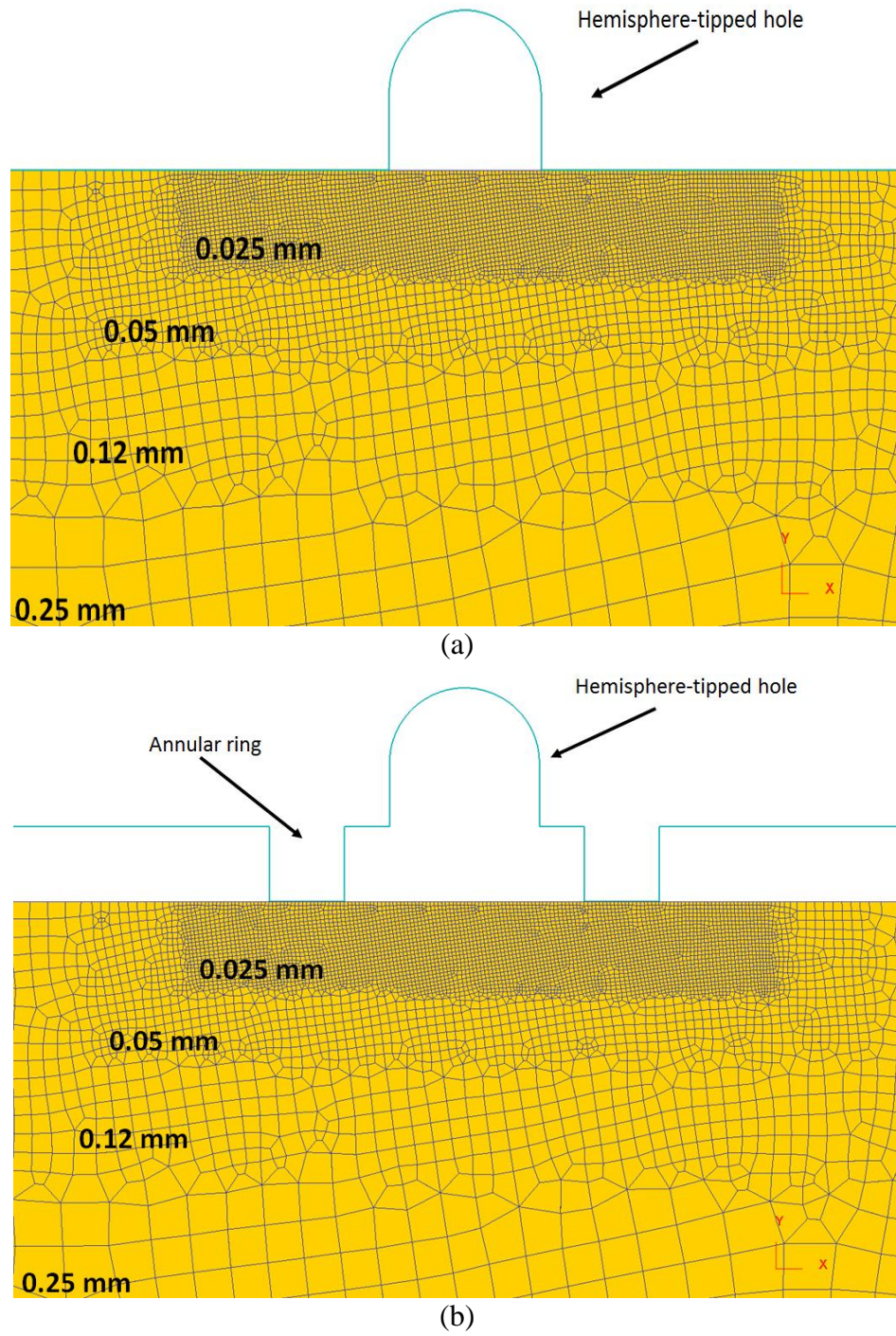


Figure 6. FEM model for the analysis of flow behavior of polymer during mold filling:

(a) hemisphere-tipped post and (b) hemisphere-tipped post with an annular ring.

The equilibrium is reached at 3000 elements. According to the results obtained from the sensitivity analysis it was recommended to work with mesh sizes above the 6000 elements. The Computer-aided engineering (CAE) model consisted of 7000 tetrahedral elements with reduced area at the points where contact and highest rates of deformation were expected. Four different density elements were designed to define the number of elements in the polymer.

The element densities used and the distribution of the elements are illustrated in Figures 6. The mesh generator of Deform-2D was used to mesh the polymer. The model consisted of 7,000 brick elements. The element sizes used within the polymer boundary were 0.25, 0.12, 0.05, and 0.025 mm as the polymer was close to the contact area with the mold features, a hemisphere-tipped hole and the alignment structure with the annular ring. A higher mesh density means that there would be more elements per unit of area compared to areas where density is lower. Higher density offers more accurate results. Figure 6(a) shows the mesh distribution for the hemisphere-tipped post and Figure 6(b) represents the mesh density for the hemisphere-tipped post with an annular ring. An Interference depth value of 8.4×10^{-3} mm was used. The equation for the calculation of the interference depth is illustrated in Equation 8 [SFTC, 2010]. Interference depth is a remesh criterion that specifies how much the slave piece, the polymer, penetrates into the master object, the mold.

$$Interference\ Depth = \frac{Smallest\ element\ size}{3} \quad (8)$$

The numerical analysis for cavity filling behavior including the analysis of the geometry, alignment structures, shape of the mold, and molding temperatures is included in the next chapter.

CHAPTER 3

DISPLACEMENT CONTROLLED SIMULATIONS

The two alignment structures, a hemisphere-tipped post and a hemisphere-tipped post with an annular ring, were modeled using a displacement control for the movement of a primary object in the numerical analysis. The displacement controlled model allows the primary object, a mold insert, to press down the polymer with a constant velocity. The flow behavior of polymer was analyzed as functions of the displacement of the mold insert and molding temperatures. Simulations were performed using plane stress boundary conditions at the molding temperatures of 75, 87.5, 100, 112.5, 125, 137.5, and 150°C. The heights of molded post were characterized depending on the molding parameters including the displacement and molding temperature.

3.1 Plane stress simulation

3.1.1 Hemisphere-tipped post

Effective stresses of polymer were observed at the bottom edge of the mold and the flow front of the polymer as shown in Figure 7. The flow stresses at the bottom edge of the mold cavity were significantly higher than the flow stress of the flow front due to the stress concentration. The flow stresses rapidly increased with the movement of the mold insert to push the polymer into the mold cavity at the beginning of mold filling. The flow stresses were 92.31 MPa and 9.96 MPa after 110 seconds, respectively as the flow front reached the boundary of the hemisphere of the mold cavity.

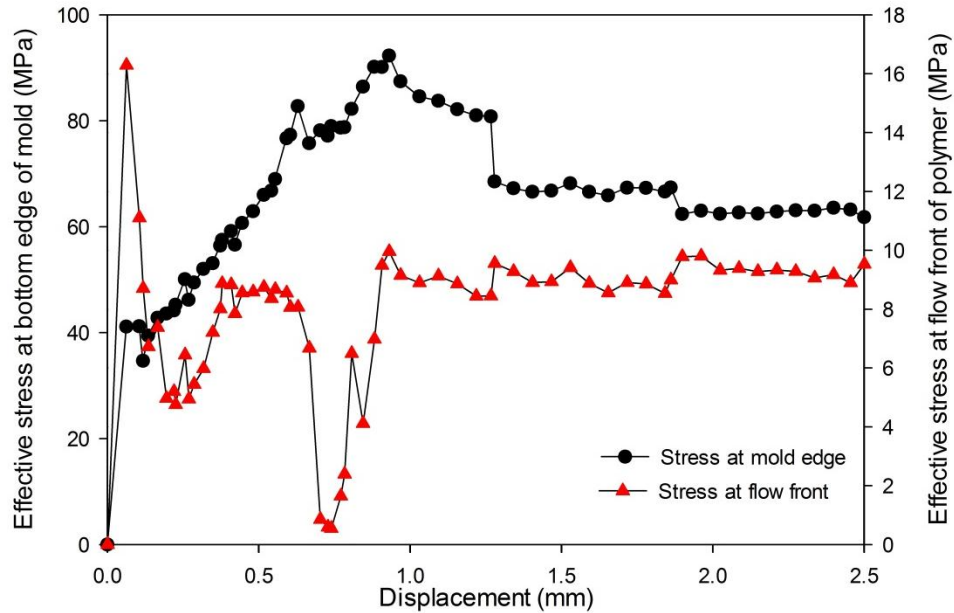


Figure 7. Stress evolution of a molded hemisphere-tipped post at the bottom edge of the mold and the flow front of polymer with a molding temperature of 87.5°C .

Figure 8 shows stress distribution of the molded hemisphere-tipped post with the increase of the displacement of the mold insert when the molding temperature was 87.5°C . The different colors in the figure represent the effective stress of polymer during mold filling. The height of mold filling with the polymer was 0.69 mm when the displacement of the mold insert was 1.0 mm as shown in Figure 8 (a). The flow front of the polymer reached at the boundary of the hemisphere-tipped cavity. Backpressure was generated due to the reduced cavity width. The effective stresses of 84.61 MPa and 8.90 MPa were obtained at the edge of the mold and the flow front of the polymer.

Figure 8 (b) shows the stress distribution with a mold displacement of 1.5 mm. The height of the molded post was 0.72 mm. Effective stress was reduced at the edge of the polymer to 68.21 MPa and increased at the flow front to 9.41 MPa caused by reduced

flow resistance at this point and the initiation of contact at the flow front of the polymer with the inner boundaries of the pattern.

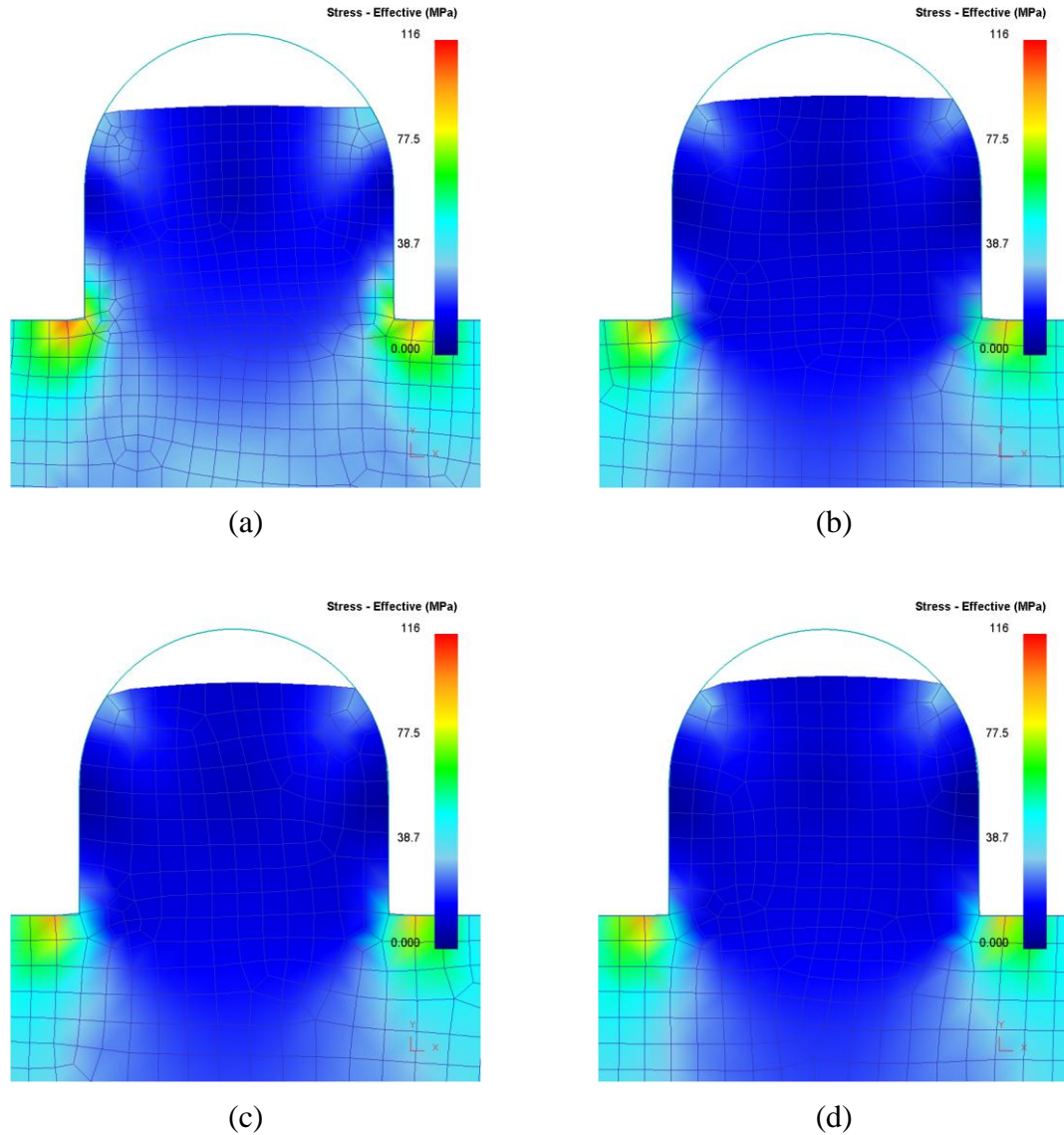


Figure 8. Stress distribution of a molded hemisphere-tipped post in mold filling while the displacement increase from 1.0 mm to 2.5 mm: (a) Mold displacement of 1.0 mm, (b) Mold displacement of 1.5 mm, (c) Mold displacement of 2.0mm, and (d) Mold displacement of 2.5mm.

The height of the molded post increased to 0.75 mm as the displacement increased from 1.5 mm to 2.0 mm as shown in Figure 8 (c). The effective stresses at the edge of the mold and flow front of the polymer were 62.47 MPa and 9.33MPa, respectively. The stress on the polymer was concentrated around the bottom edge of the mold cavity throughout the mod filling. This can induce excessive residual stress and defects on the molded structure. Figure 8 (d) shows incomplete mold filling with polymer. It is the furthest that the flow front of the polymer advanced into the cavity at the molding temperature of 87.5°C and with the displacement of 2.5 mm.

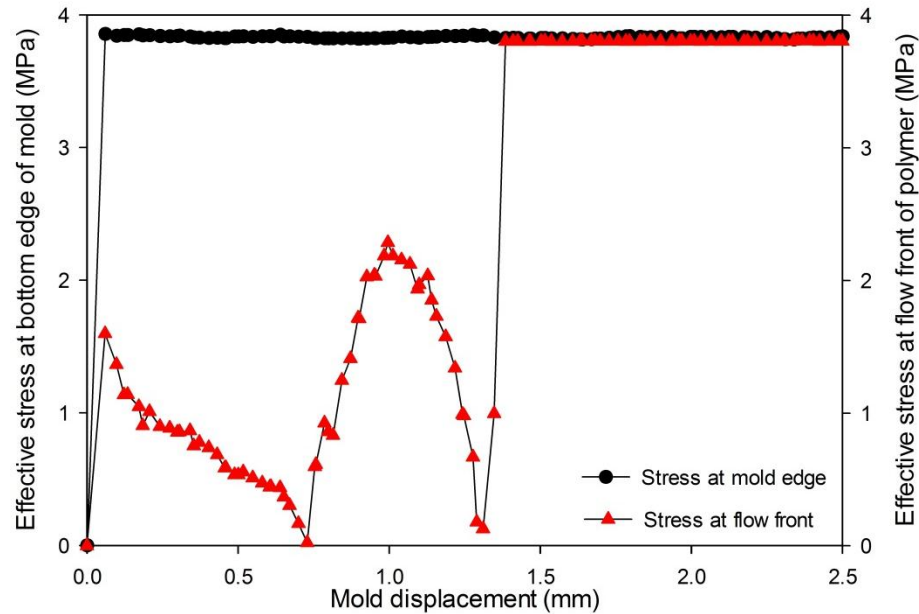


Figure 9. Stress evolution of a molded hemisphere-tipped post at the bottom edge of the mold and the flow front of polymer with a molding temperature of 112.5°C.

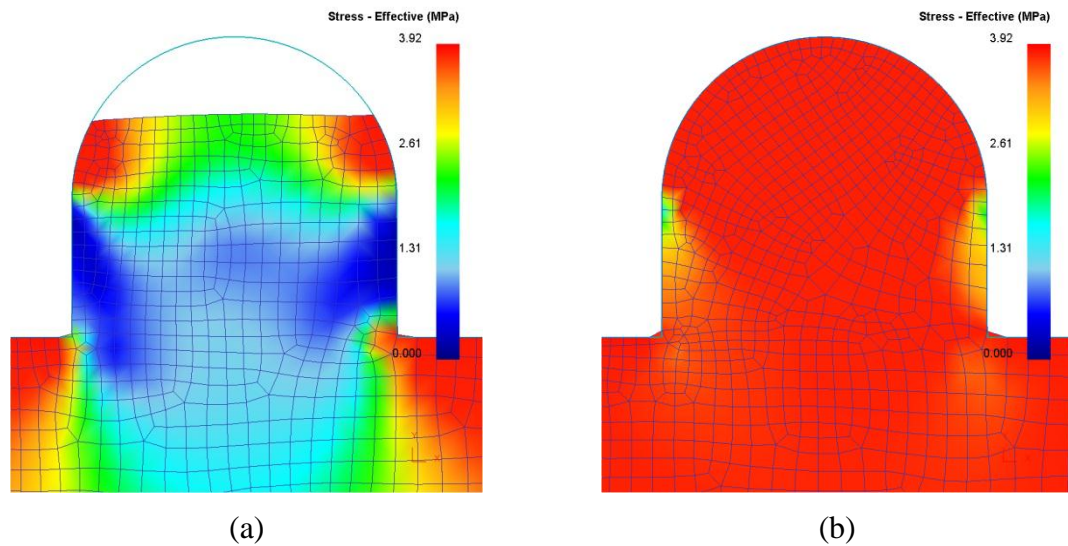


Figure 10. Stress distribution of a molded hemisphere-tipped post in mold filling while the displacement increase from 1.0 mm to 2.5 mm: (a) Mold displacement of 1.0 mm and (d) Mold displacement of 2.5 mm.

Figure 10 shows the effective stress distribution of a hemisphere-tipped post at a molding temperature of 112.5°C. The mold filling height of 0.68 mm was achieved with the displacement of 1.0 mm as shown in Figure 10 (a).

The highest effective stress points are located at the bottom edge of the mold. Figure 3.4 shows the effective stress distribution of a hemisphere-tipped post at a molding temperature of 112.5°C. The mold filling height of 0.68 mm was achieved with the displacement of 1.0 mm as shown in 10 (a). The highest effective stress points are located at the bottom edge of the mold. The increase of the stress at the flow front was resulted from the increased fluidic resistance with the reduced cavity width at the hemisphere. The mold cavity was completely filled at the displacement of 1.5 mm of displacement with the molding time of 178.81 seconds as shown in Figure 10 (b). Effective stresses in both reference points were around 3.83 MPa.

Figure 11 shows the evolution of effective stresses in mold filling at a molding temperature of 150°C. Polymer flow behavior was different at every temperature used, the trend observed showed that the higher the temperature the lower the stress suffered by the polymer substrate.

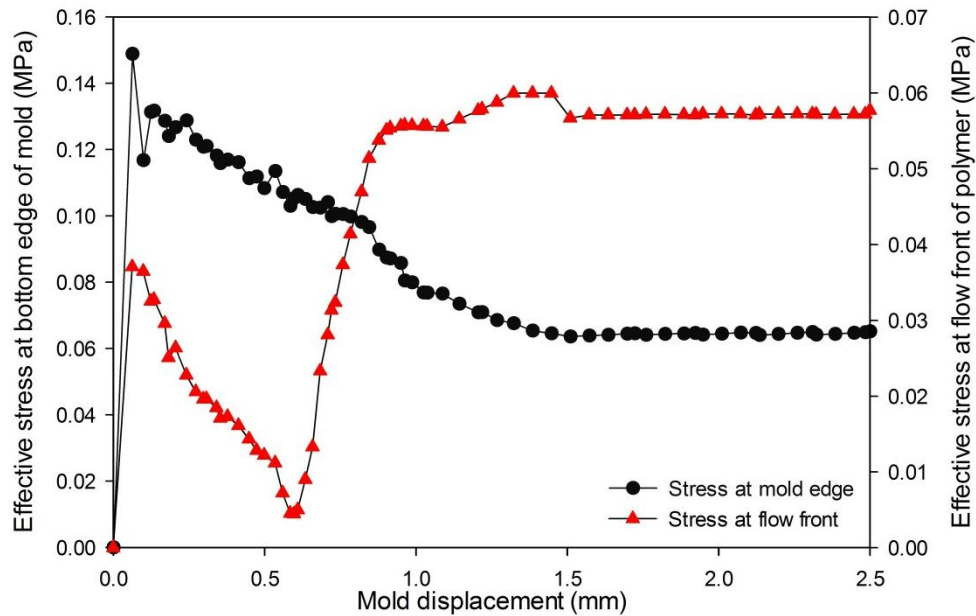


Figure 11. Stress evolution of a molded hemisphere-tipped post at the bottom edge of the mold and the flow front of polymer with a molding temperature of 150°C.

The flow front of the polymer showed a rapidly increase in pressure up to 0.03 MPa while the polymer surmounted the flow resistance, decreasing to 0.004 MPa before it reached the pattern's boundary. Once the flow front reached that point the effective stress increased to 0.06 MPa maintaining it constant after the cavity was completely filled.

Stress evolution at the edge of the mold was completely different than the behavior observed at the flow front stress evolution. The difference between the two reference points is caused mainly because this point was always in direct contact with the

top die. The flow resistance at this point was higher and a stress of 0.14 MPa was observed at the moment the polymer initiated to fill the cavity.

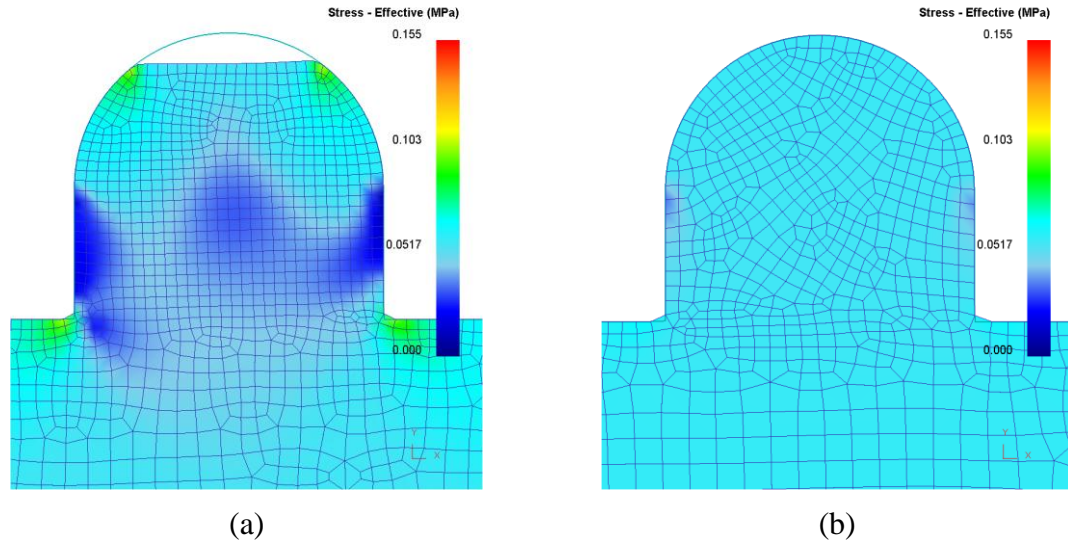


Figure 12. Stress distribution of a molded hemisphere-tipped post in mold filling while the displacement increase from 1.0 mm to 2.5 mm: (a) Mold displacement of 1.0 mm and (b) Mold displacement of 1.5 mm

Pressure began to decrease after this point to 0.06 MPa where it was observed constant after the cavity was completely filled. Having equal stresses at both reference points after the complete filling of the pattern means that the mold is still applying pressure but the polymer is now spreading to the sides since there is no other place to go into the hemisphere-tipped cavity.

A mold displacement of 1.0 mm reached a filling height of 0.82 mm as presented in Figure 12 (a). This filling height is exactly 0.14 mm higher than the filling height obtained with a molding temperature of 112.5°C demonstrating that the polymer is flowing easily at higher temperatures and with reduced effective stress. After 1.5 mm of mold displacement the cavity was completely filled as shown in Figure 12 (b).

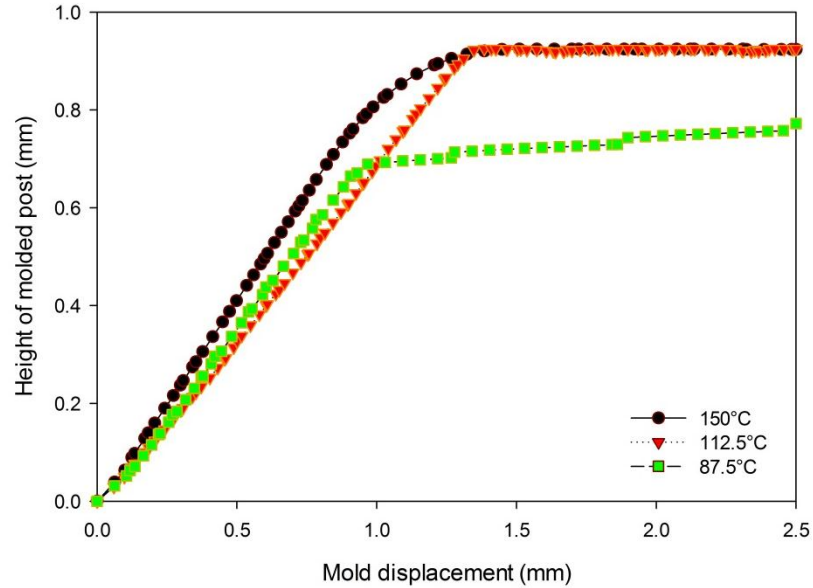


Figure 13. Heights of the molded posts at the molding temperatures of 87.5, 112.5, and 150°C when the displacement increased from 0.5 mm to 2.5 mm.

Higher embossing temperatures not only reduce the effective stress on the polymer substrate but also provide elevated filling velocities to the molding process. Figure 13 shows the heights of the molded posts as functions of the mold displacement and molding temperatures. A molding temperature of 150°C showed the most significant results regarding filling behavior requiring only 172.35 seconds and a total mold displacement of 1.38 mm. results observed with an embossing temperature of 112.5 °C confirmed that higher temperatures resulted in reduced filling times. To completely fill the hemisphere-tipped cavity at 112.5 °C a total top die displacement of 2.20 mm and an embossing time of 275.11 seconds were required.

Process parameters with molding temperatures below T_g failed to fill completely fill the hemisphere-tipped cavity. A molding temperature of 87.5 °C reached a post height of 0.77 mm after 300 seconds of embossing. Effective stress was reduced as well with the

increment in molding temperatures. Pressure was reduced from 61.85 MPa at 87.5 °C to 0.06 MPa at 150 °C.

3.1.2 Hemisphere-tipped post with an annular ring

Figure 14 shows the stress evolution of the hemisphere-tipped post at the molding temperature of 87.5°C. The effective stress at the bottom edge of mold is higher than at the flow front of the polymer. The maximum effective stress was 114.4 MPa at the edge of the mold.

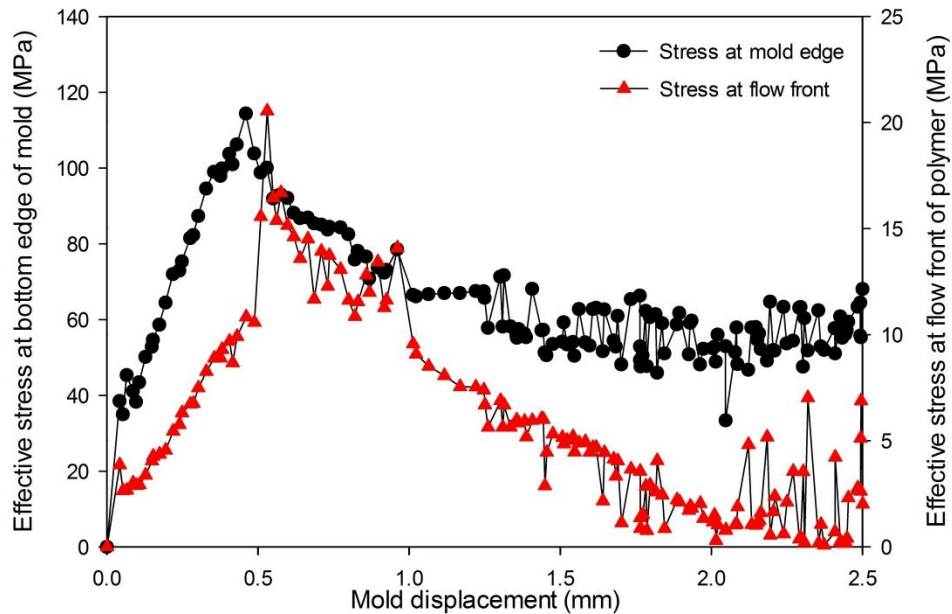


Figure 14. Stress evolution of a molded hemisphere-tipped post with an annular ring at the bottom edge of the mold and the flow front of polymer with a molding temperature of 87.5°C.

An additional annular ring was proposed to assist the mold filling with the polymer for the fabrication of a reliable hemisphere-tipped post [Chen et al., 2007].

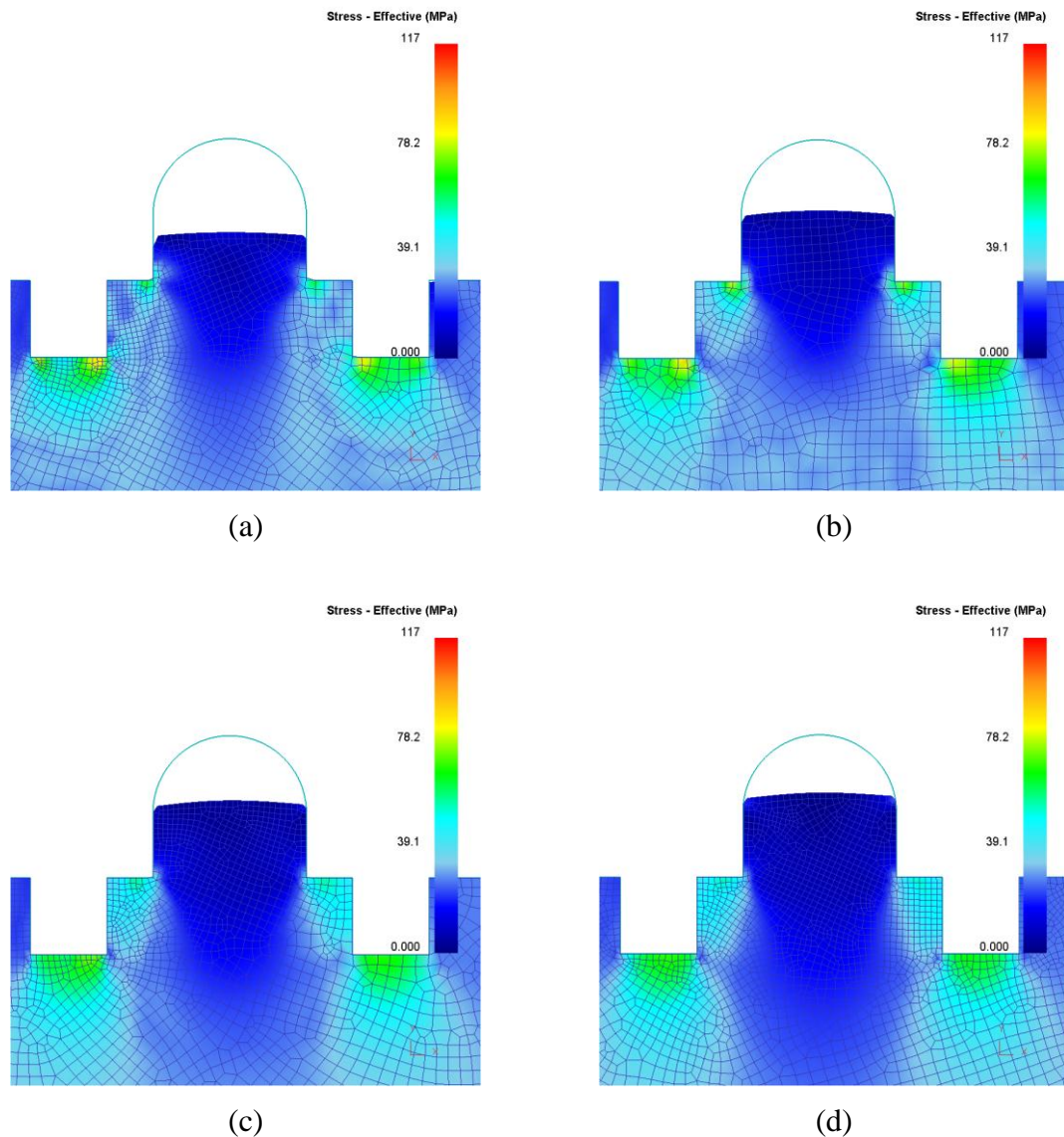


Figure 15. Stress distribution of a molded hemisphere-tipped post with an annular ring in mold filling while the displacement increase from 1.0 mm to 2.5 mm: (a) Mold displacement of 1.0 mm, (b) Mold displacement of 1.5 mm, (c) Mold displacement of 2.0mm, and (d) Mold displacement of 2.5 mm

The flow front had the effective stress varied from 0 MPa to 21 MPa in mold filling. The stress evolution of a hemisphere-tipped post with the ring was represented in Figure 15. A mold displacement of 1.0 mm achieved a mold filling height of 0.81 mm at

an embossing time of 118 seconds as shown in Figure 15 (a). The stress concentration was observed at the bottom edge of the mold. It was 78.13 MPa while the front flow of the polymer had a stress of 11.55 MPa.

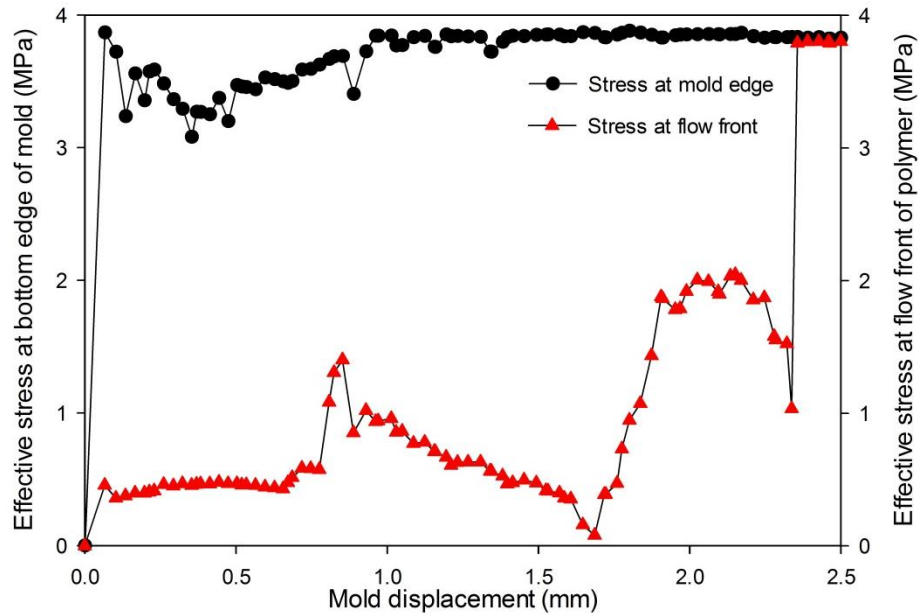


Figure 16. Stress evolution of a molded hemisphere-tipped post with an annular ring at the bottom edge of the mold and the flow front of polymer with a molding temperature of 112.5°C.

The polymer substrate was not able to fill entirely the hemisphere-tipped hole with a molding temperature of 87.5 °C as well as observed with the first alignment structure. Figure 15 (b) shows concentrated stress of 65.78 MPa at the bottom edge of the mold. A total mold displacement of 2.0 mm is observed in Figure 15 (c). The height of the molded post at this point was 1.00 mm after 239 seconds of embossing.

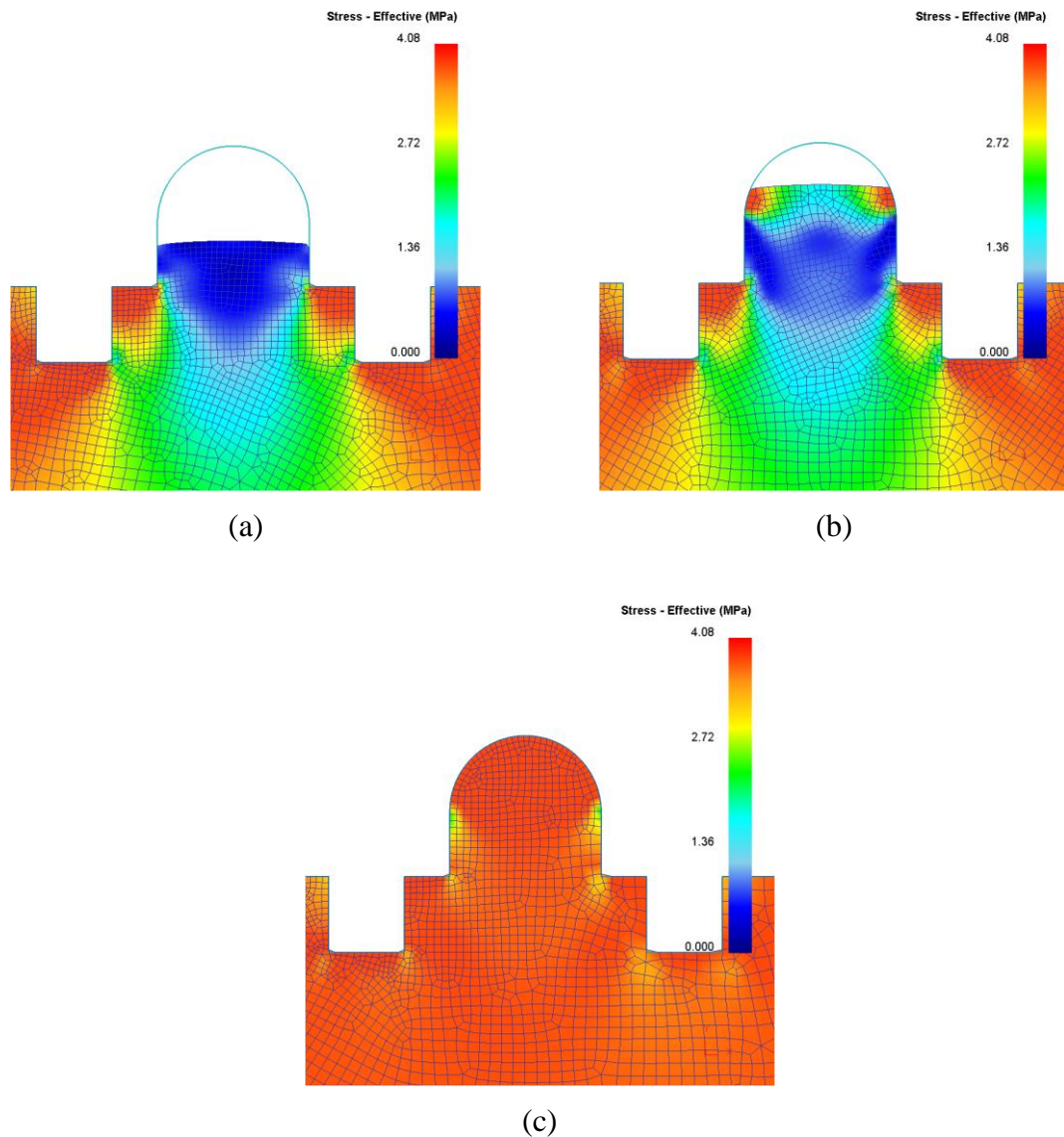


Figure 17. Stress distribution of a molded hemisphere-tipped post with an annular ring in mold filling while the displacement increase from 1.0 mm to 2.5 mm: (a) Mold displacement of 1.0 mm, (b) Mold displacement of 1.5 mm, and (c) Mold displacement of 2.0mm.

A total polymer displacement of 1.05 mm was achieved with a displacement of 2.5 mm and 300 seconds of molding time as shown in Figure 15 (d).

A molding temperature of 87.5°C considered a low process temperature that might generate higher rates of stress in the polymer substrate affecting the pattern quality of the finished product. The evolution of effective stress of the hemisphere-tipped post with the ring was shown in Figure 16. The molding temperature was 112.5°C . The stress at the edge of the mold ranged from 3.0MPa to 3.8MPa.

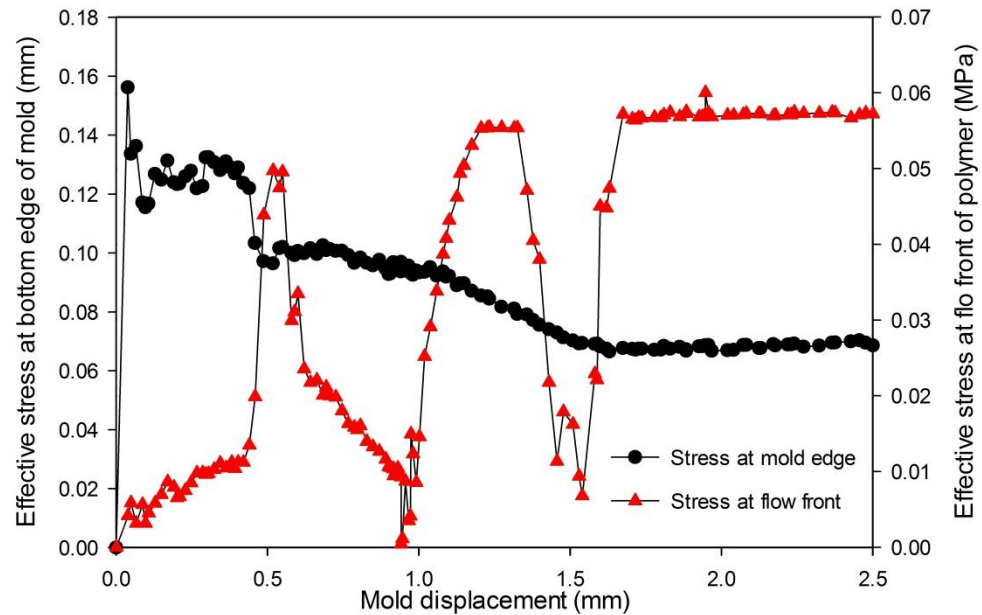


Figure 18. Stress evolution of a molded hemisphere-tipped post with an annular ring at the bottom edge of the mold and the flow front of polymer with a molding temperature of 150°C .

Effective stress distribution of the cavity filling process with different mold displacements is shown in Figure 17. A total mold displacement of 1.0 mm shows an increase in pressure up to 3.84 MPa at the edge of the mold as illustrated in Figure 17 (a). Figure 17 (b) shows a post height of 1.15 mm observed after 180.54 seconds of embossing and a total mold displacement of 1.5 mm. The polymer reached the inner radius of the hemisphere-tipped hole at an effective stress of 1.78 MPa. The cavity was

completely filled using less than 2.0 mm of mold displacement and around 236 seconds of embossing time. After 300 seconds of embossing time the mold reached 2.5 mm of displacement and effective stress was stable in both reference points around 3.80 MPa.

A molding temperature of 150°C was used in Figure 18. Effective stress was reduced to similar rates observed in the first structure under the same process parameters. The effective stress observed at the edge of the mold maintained values between 0.06 and 0.10 MPa.

The inflection points observed on the flow front of the polymer trend line may be caused by slipping of the polymer inside the mold and also by the pass of the polymer in certain areas of the mold.

Effective stress distribution is represented in Figure 19. A mold displacement of 1.0 mm resulted with a filling height of 0.92 mm. Figure 19(a) illustrates an embossing time of 121.13 seconds. Effective stress at the edge of the mold is 0.10 MPa and at the flow front of the polymer is 0.01 MPa. After 181.91 seconds of embossing time the filling height of the polymer was around 1.31 mm as shown in Figure 19(b).

The results observed show that the increase in temperature also increased the filling height of the polymer. The total embossing time was 297.45 seconds. At this time the mold reached 2.5 mm of displacement and the simulation was terminated. At the end of the molding process both reference points reached equilibrium at 0.06 MPa.

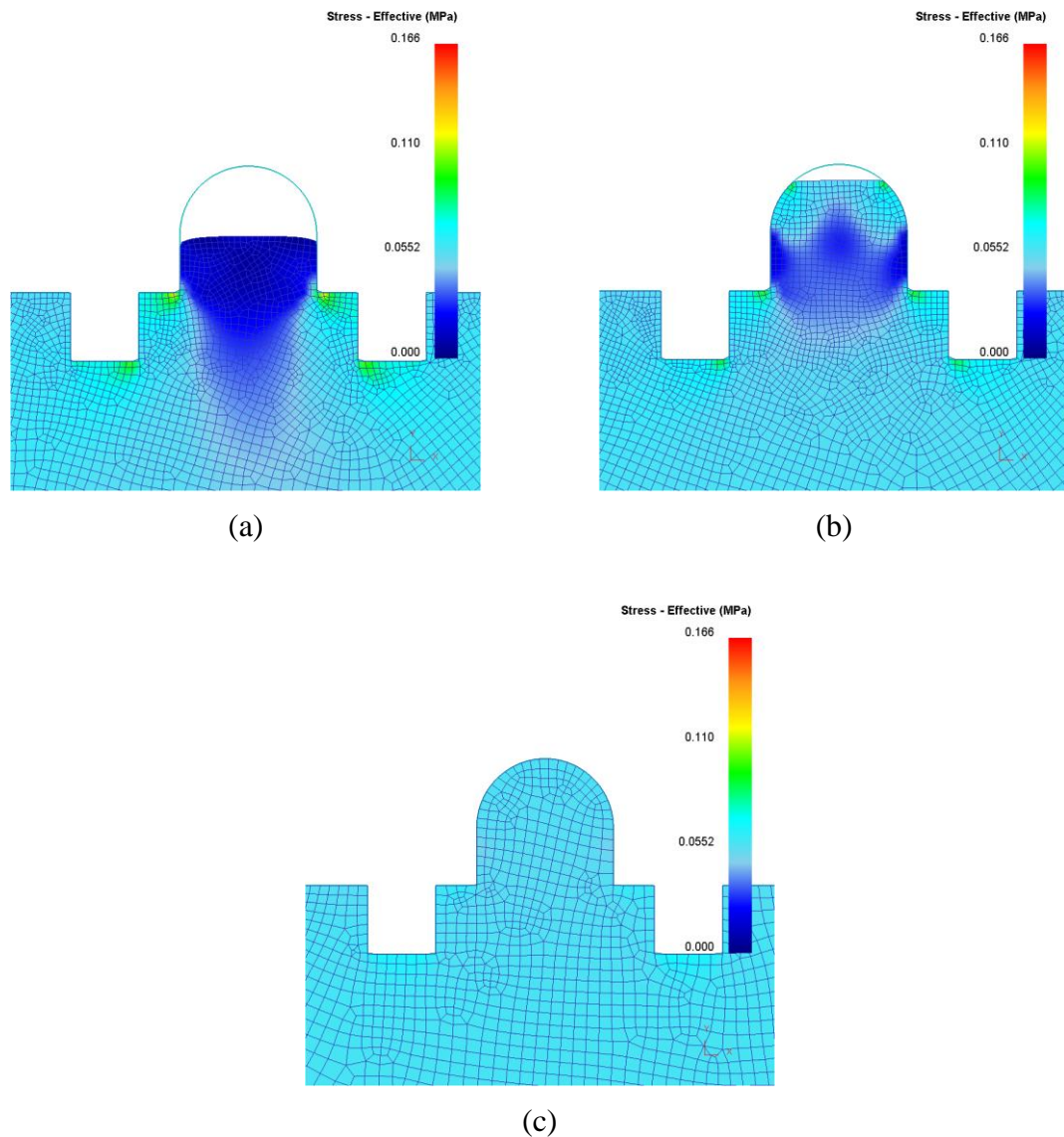


Figure 19. Stress distribution of a molded hemisphere-tipped post with an annular ring in mold filling while the displacement increase from 1.0 mm to 2.5 mm: (a) Mold displacement of 1.0 mm, (b) Mold displacement of 1.5 mm, and (c) Mold displacement of 2.0mm.

The relationship between the height of the molded post and the total displacement of the top die at three different molding temperatures is shown in Figure 20. It was observed that a molding temperature of 150 °C presented the fastest filling behavior

requiring 1.58 mm of mold displacement to fill the cavity, compared to the 1.61 mm used with an embossing temperature of 112.5 °C. A mold temperature of 87.5 °C failed to fill the cavity generating elevated stress that could cause defects on the terminated product.

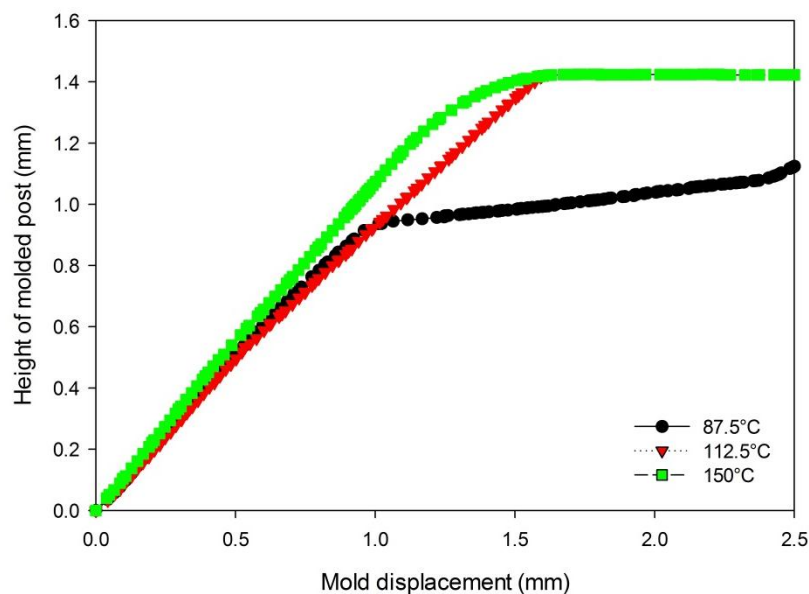


Figure 20. Heights of the molded posts at the molding temperatures of 87.5, 112.5, and 150°C when the displacement increased from 0.5 mm to 2.5 mm.

There is a small difference in the mold displacement used to complete the hemisphere-tipped cavity at 112.5 and 150 °C. However, the biggest difference was observed on the filling times where at 112.5 °C it took the polymer 245.12 seconds to fill the cavity versus the 224.45 seconds required at 150 °C.

3.2 Chapter conclusion

The increase in the embossing temperature promoted a faster cavity filling by a reduction in effective stress and flow resistance. Less flow resistance allowed the polymer substrate to flow easier into the hemisphere-tipped hole. Temperatures below T_g failed to completely fill the cavity. Signs of damage were observed in the cavity filling of

a hemisphere-tipped post with an annular ring below the glass transition temperature.

This means that under those process parameters the quality of the pattern is affected by the excessive pressure.

CHAPTER 4

FORCE CONTROLLED SIMULATIONS

Force controlled simulations are based on a specified load applied directly on the surface of the top die. The applied load will move the top die downwards applying pressure on the polymer substrate forcing it to flow into the hemisphere-tipped hole filling the cavity. This chapter presents the simulation conditions used for the force controlled analysis, the simulation model for the alignment structures, and the results obtained from the numerical simulation under force controlled analysis. Different molding temperatures were included along with several embossing loads to analyze the behavior of the polymer during cavity filling under these process parameters.

4.1 Simulation conditions

Forces of 300, 600, and 900 N were applied to the polymer substrate for a period of 5 seconds. To avoid the damping effect a hydraulic press behavior was simulated. The damping phenomena occur when the mold is unable to penetrate into the polymer substrate making it bounce on the surface. The force was applied gradually as an approximation to the displacement of a hydraulic press as presented in Figure 21. The load was zero at the beginning of the simulation and was gradually increase up to half the total load at 0.5 seconds of molding time. When the simulation reached the 1st second of molding the force was totally applied. A holding time of 4 seconds was added to the simulation. The holding time is the part of the molding process where the press will maintain constant pressure on over the polymer substrate.

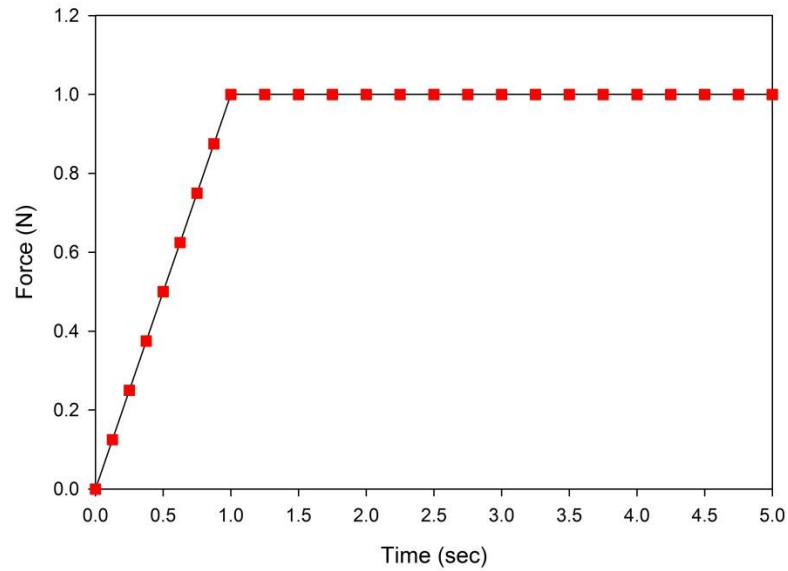


Figure 21. Application of the load depending on molding time.

A schematic representation of the simulation model is represented in Figure 22.

The numerical analysis included forces of 300, 600, and 900 N. Two alignment structures were used: a hemisphere-tipped post and a hemisphere-tipped post with an annular ring.

The geometry and dimension for the alignment structures was defined in previous chapters. Molding temperatures of 75, 87.5, 100, 112.5, 125, 137.5, and 150°C were included in the numerical analysis.

Force Controlled Simulations																	
Axisymmetric																	
Hemisphere-tipped post									Hemisphere-tipped post with an annular ring								
300 N			600 N			900 N			300 N			600 N			900 N		
T ₁	T ₂	T ₃	T ₁	T ₂	T ₃	T ₁	T ₂	T ₃	T ₁	T ₂	T ₃	T ₁	T ₂	T ₃	T ₁	T ₂	T ₃

Figure 22. Force controlled matrix at T1 = 87.5°C, T2 = 112.5, and T3 = 150°C

4.2 Axisymmetric simulation

Axial-symmetric geometry was used to simulate the polymer behavior in the filling of a hemisphere-tipped post and a hemisphere-tipped post with an annular ring. Three molding pressures were applied to the model to analyze the difference in effective stress and molding times. Molding temperatures, filling heights, mold displacements and embossing forces were used to understand the polymer flow behavior.

4.2.1 Hemisphere-tipped post

This alignment structure was used first as the basic approach to understand polymer flow behavior. The analysis of the structure is explained based on the results obtained from the effective stress curves, effective stress distribution figures that show how the polymer flow into the cavity, the effect of embossing pressures and molding temperatures on the polymer substrate and the mold displacement required to fill cavity.

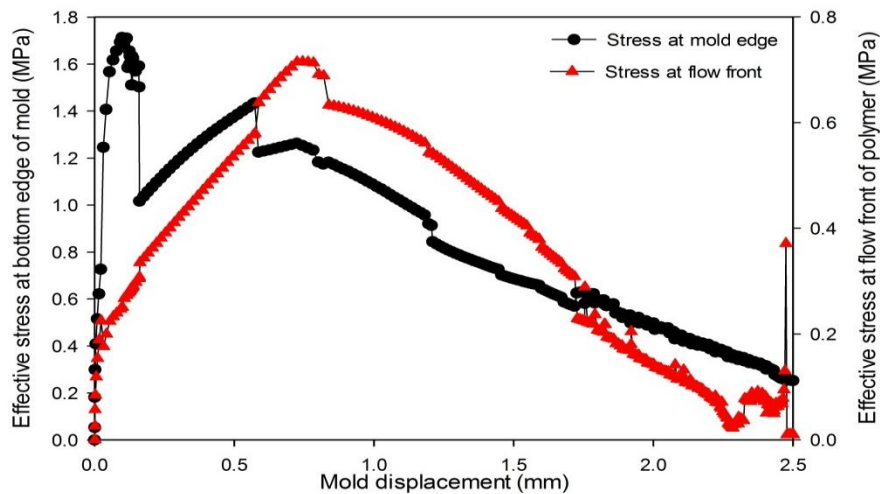


Figure 23. Stress evolution of a molded hemisphere-tipped post at the bottom edge of the mold and the flow front of polymer with a molding temperature of 150°C and a molding force of 300 N.

An embossing process of a hemisphere-tipped post using a molding force of 300N did not caused any deformation at all on the polymer substrate using molding temperatures below T_g . In fact; deformation was only observed using a molding temperature of 150°C. Figure 23 illustrates the effective stress evolution at an embossing temperature of 150°C and a molding force of 300 N.

The effective stress at the edge of the mold shows its highest pressure point at 1.72 MPa after 0.1 seconds of embossing. After that point pressure decreased due to the reduced flow resistance. The flow fronts of the polymer shows its highest pressure point at 0.72 MPa when the polymer reached the inner radius of the hemisphere-tipped hole. Both reference points present similar behavior with higher pressure at the edge of the mold. Effective stress distribution is presented in Figure 4.4. Total mold displacements of 1.0, 1.5, 2.0, and 2.5 mm are illustrated in the figure. Under a mold displacement of 1.0 mm a filling height of 0.25 mm was observed. Figure 24(a) shows the effective stress distribution at this point.

Effective stresses of 0.43 and 0.69 MPa were observed at the flow front of the polymer and at the edge of the mold respectively and are illustrated in Figure 24(b). Pressure is higher at the edge of the mold and is spreading towards the center of the polymer substrate. A filling height of 0.59 mm is represented in Figure 24(c).

The effective stress at the flow front of the polymer is reduced to 0.14 MPa and 0.50 MPa at the edge of the mold. Figure 24(d) shows the cavity completely filled after 2.55 seconds of embossing. To achieve the complete filling of the hemisphere-tipped post it was necessary a mold displacement of 2.47 mm. Effective stress under these process

parameters was considered higher compared to the simulation results obtained from displacement controlled simulations.

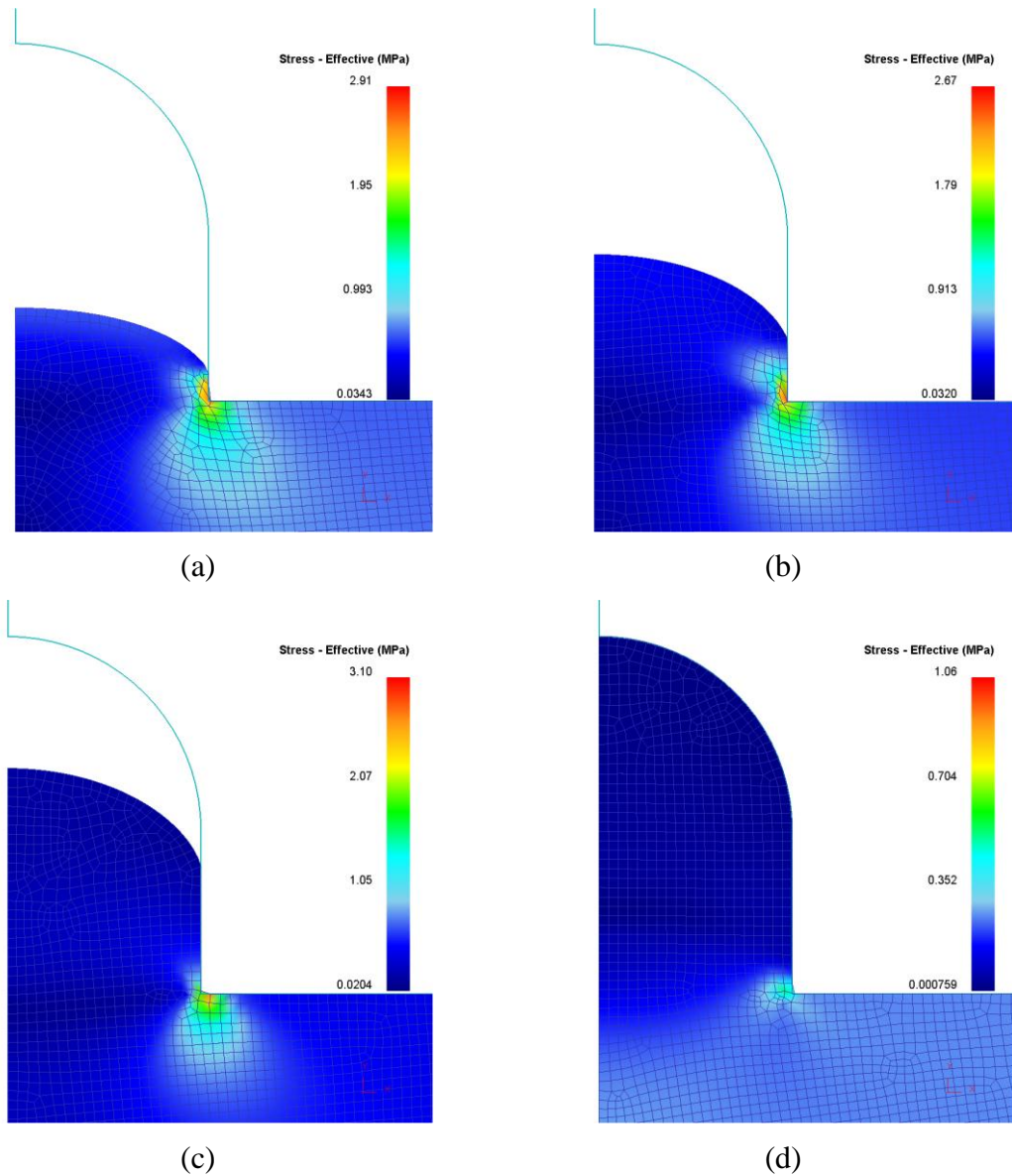


Figure 24. Stress distribution of a molded hemisphere-tipped post in mold filling while the displacement increase from 1.0 mm to 2.5 mm: (a) Mold displacement of 1.0 mm, (b) Mold displacement of 1.5 mm, (c) Mold displacement of 2.0mm, and (d) Mold displacement of 2.5mm.

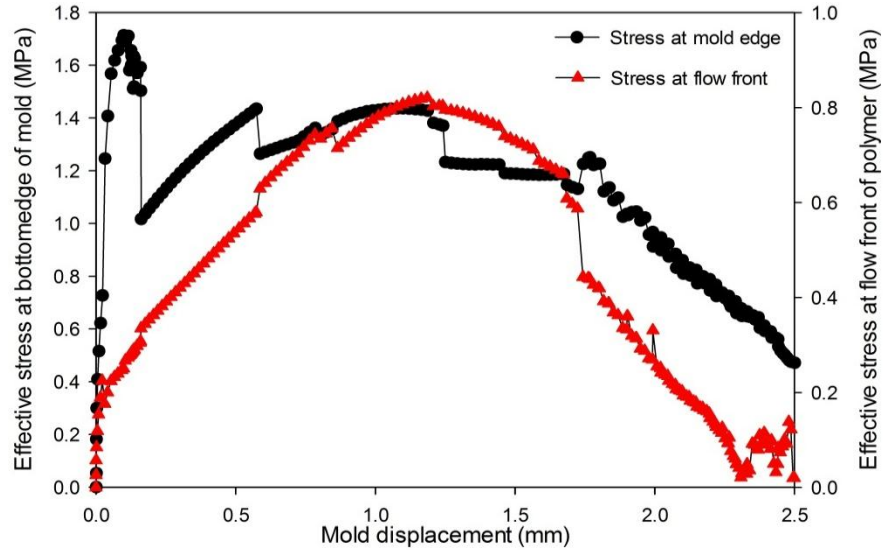


Figure 25. Stress evolution of a molded hemisphere-tipped post at the bottom edge of the mold and the flow front of polymer with a molding temperature of 150°C and a molding force of 600 N.

Effective stress evolution under an embossing force of 600 N is shown in Figure 4.5. The highest pressure point at the mold edge is located at 1.72 MPa and is caused by the polymer initiating to flow into the hemisphere-tipped hole. The flow front of the polymer shows its highest effective stress point at the moment the polymer substrate reaches the inner radius of the structure. The reduction in area increases the flow resistances reflected in effective stress.

Effective stress distribution under a molding force of 600 N is presented in Figure 4.6. An effective stress of 1.43 MPa is observed at the edge of the mold. Pressure is expanding towards the center of the polymer substrate with higher effective stress at the places in direct contact with the top die as illustrated in Figure 26(a).

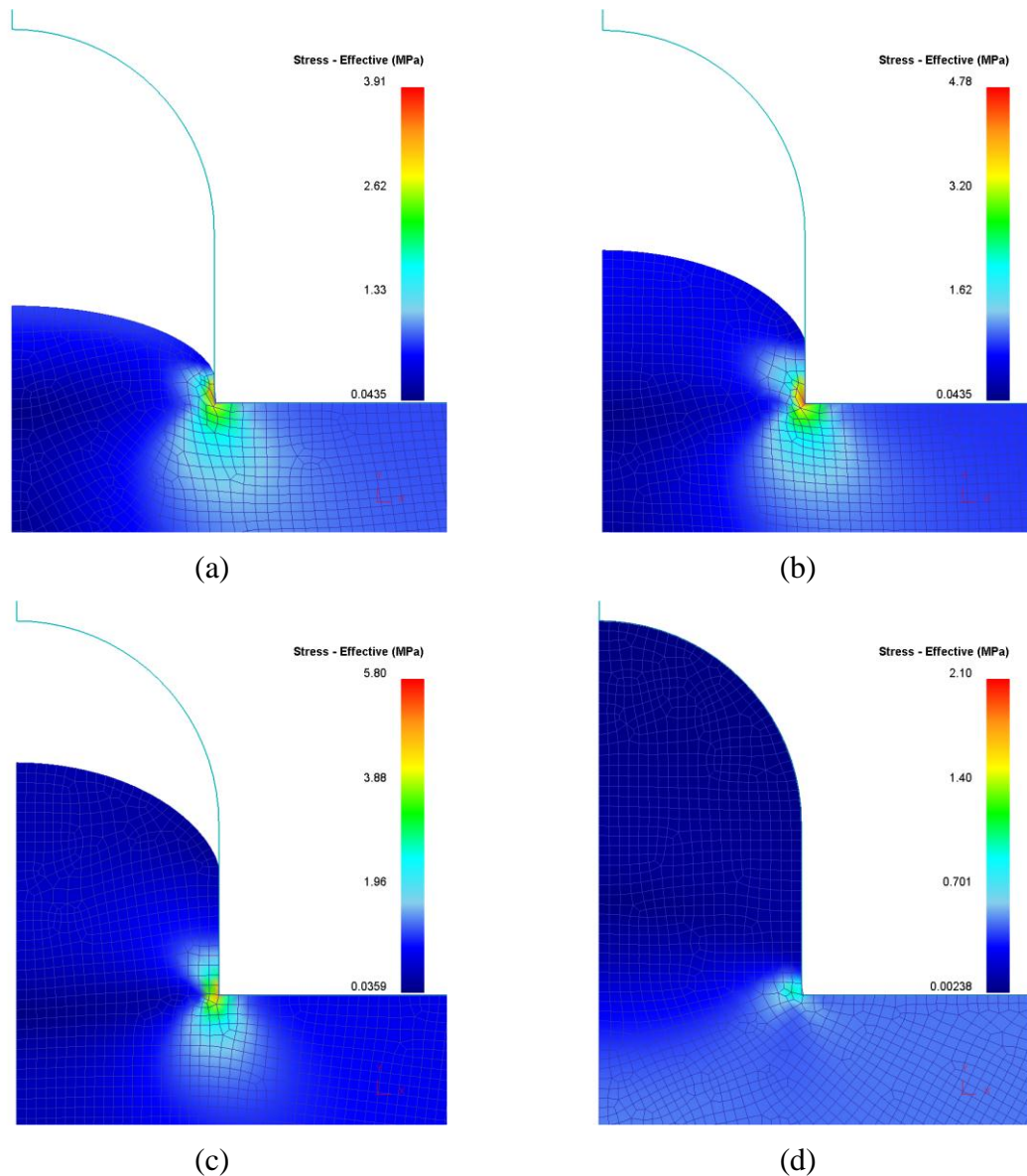


Figure 26. Stress distribution of a molded hemisphere-tipped post in mold filling while the displacement increase from 1.0 mm to 2.5 mm: (a) Mold displacement of 1.0 mm, (b) Mold displacement of 1.5 mm, (c) Mold displacement 2.0 of 2.0mm, and (d) Mold displacement of 2.5 mm.

Effective stress is spreading from the edge of the mold into the inner wall of the structure as represented in Figure 26(b). A reduction in effective stress is observed in Figure 26(c) concentrating in the edge of the mold at 0.94 MPa. The structure was

completely filled in figure 26(d) after 1.62 MPa seconds and a total die displacement of 2.48 mm.

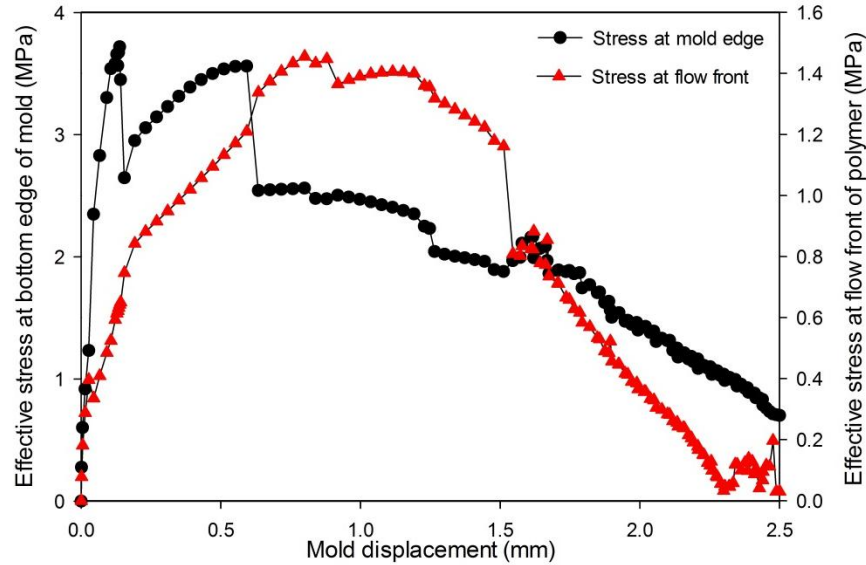


Figure 27. Stress evolution of a molded hemisphere-tipped post at the bottom edge of the mold and the flow front of polymer with a molding temperature of 150°C and a molding force of 900 N.

A molding force of 900 N was able to cause polymer deformation at 150°C. Effective stress evolution is illustrated in Figure 27. The flow front of the polymer shows a similar behavior to the one observed at lower embossing forces. The highest effective stress point is observed when the polymer reaches the inner radius of the structure. The highest effective stress point at the edge of the mold is caused by the polymer initiating to flow into the hemisphere-tipped hole. The distribution of effective stress is illustrated in Figure 28.

Passed 0.30 seconds of embossing the polymer reached a height of 0.24 mm under an effective stress of 2.47 MPa at the edge of the mold as shown in Figure 28(a).

The decrease in effective stress at the flow front of the polymer is represented in Figure 28(b).

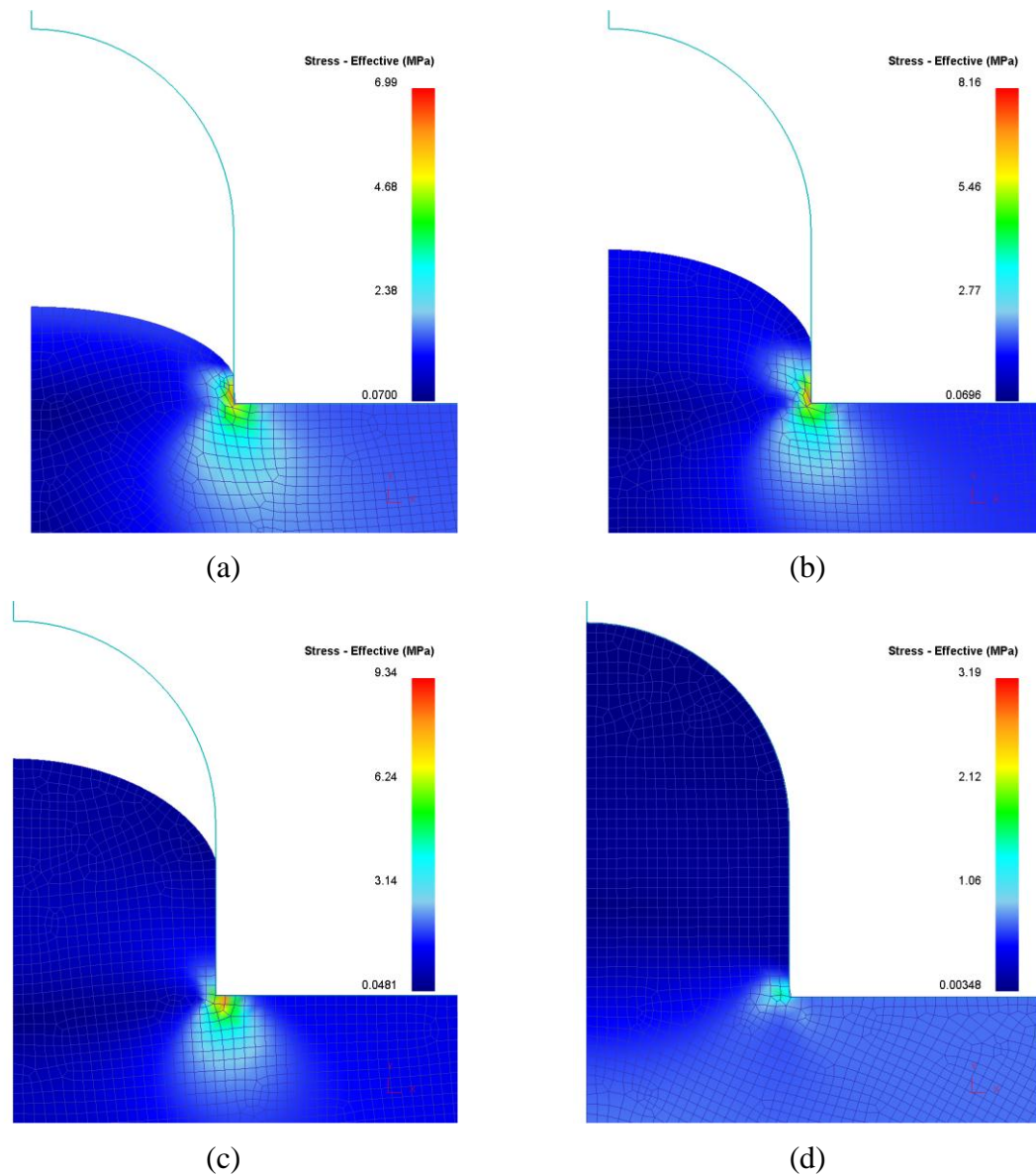


Figure 28. Stress distribution of a molded hemisphere-tipped post in mold filling while the displacement increase from 1.0 mm to 2.5 mm: (a) Mold displacement of 1.0 mm, (b) Mold displacement of 1.5 mm, (c) Mold displacement of 2.0mm, and (d) Mold displacement of 2.5 mm.

During the remaining time of the molding process the effective stress continued decreasing as illustrated in Figure 28(c) and locating the highest pressure points at the edge of the mold. Figure 28(d) presents the cavity completely filled after 0.90 seconds of embossing. To complete the structure a total mold displacement of 2.47 mm was required.

A comparison between the height of the molded post and the molding temperature is shown in Figure 29. Temperatures below T_g failed to produce any deformation on the polymer substrate at all embossing forces used in the numerical analysis. The pressure used in the numerical analysis was considered low to produce deformation to the polymer substrate. It was noticed that a molding force of 900 N was the fastest of them all.

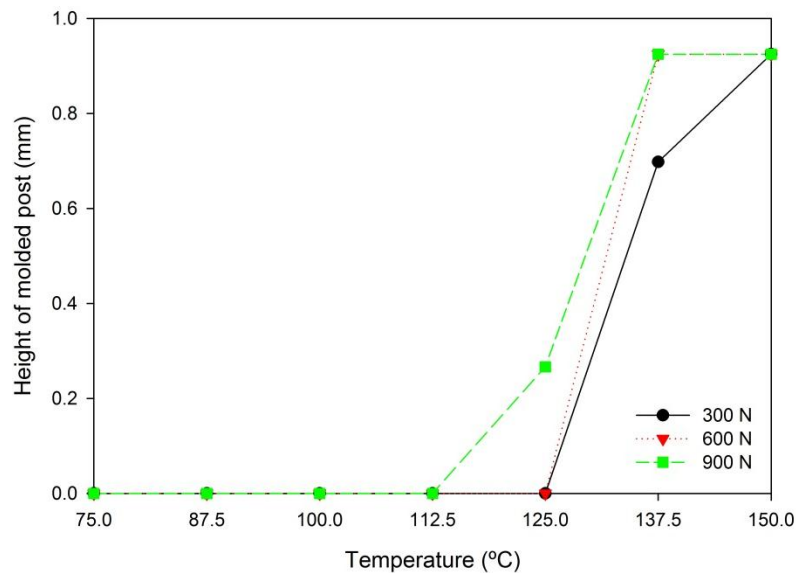


Figure 29. Heights of the molded posts at the molding temperatures of 87.5, 112.5, and 150°C when the displacement increased from 0.5 mm to 2.5 mm.

There were no significant differences in the mold displacement required to complete the alignment structure at the embossing forces included in the numerical analysis. However, the time required to fill the cavity was reduced with the force

increment. Effective stress was increased with the intensification of embossing force as expected.

4.2.2 Hemisphere-tipped post with an annular ring

The second alignment structure included in the numerical analysis was a hemisphere-tipped post with an annular ring. The alignment structure was tested under the same process parameters as the previous structure. Polymer flow behavior was analyzed depending on the imprinted pattern in the mold.

The effective stress evolution during the cavity filling of a hemisphere-tipped post with an annular ring at 112.5°C and a molding force of 300 N is illustrated in Figure 30.

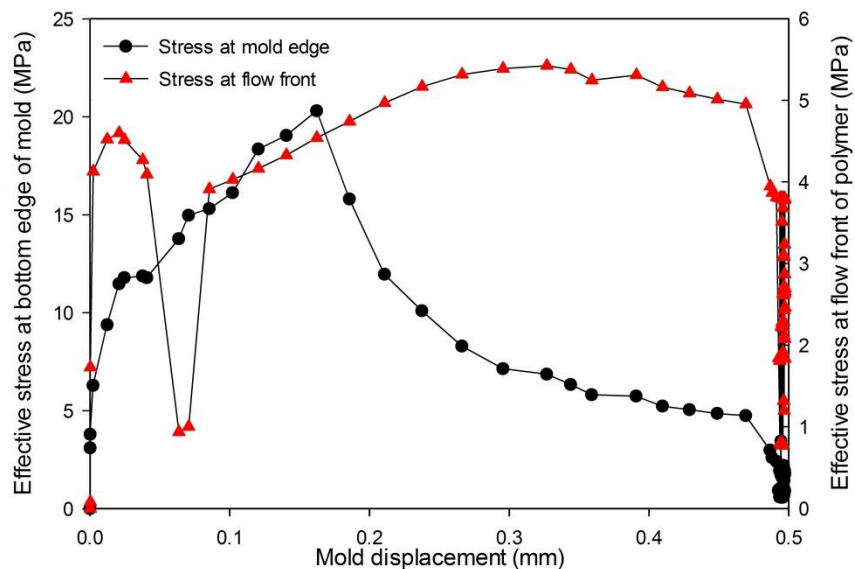


Figure 30. Stress evolution of a molded hemisphere-tipped post with an annular ring at the bottom edge of the mold and the flow front of polymer with a molding temperature of 112.5°C and a molding force of 300 N.

The flow front of the polymer illustrates an increase in pressure at the beginning of the molding process. The effective stress at the edge of the mold increased up to 20 MPa during the initial 0.20 mm of mold displacement.

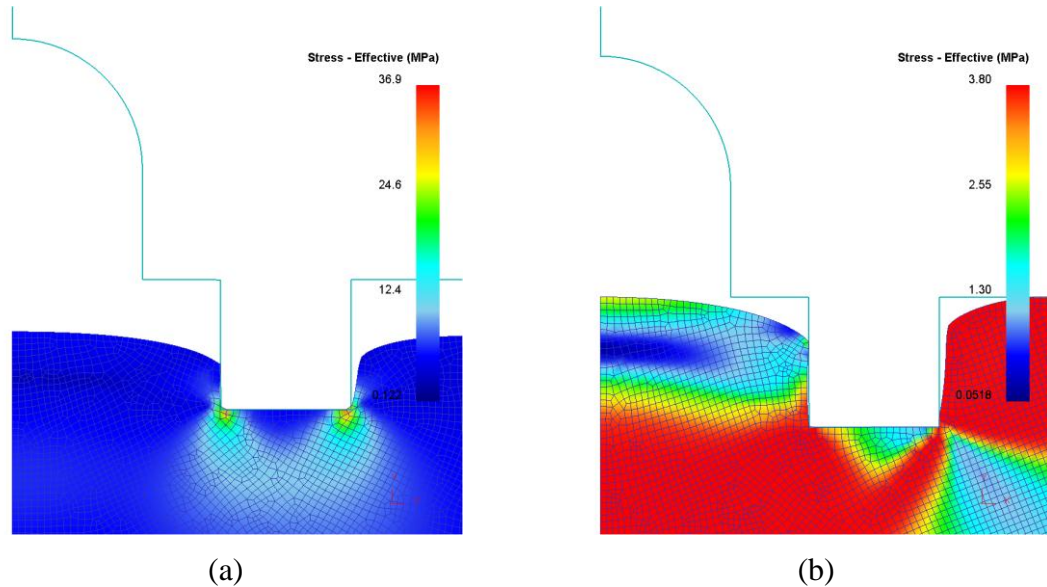


Figure 31. Stress distribution of a molded hemisphere-tipped post in mold filling while the displacement increase from 0.25 mm to 0.50 mm: (a) Mold displacement of 0.25 mm and (b) Mold displacement of 0.5 mm.

An embossing force of 300 N and a molding temperature of 112.5°C failed to fill the hemisphere-tipped hole as shown in Figure 31. The molding time was completed resulting in a total die displacement of 0.5 mm.

The effective stress distribution after 0.07 seconds of embossing is illustrated in Figure 31(a). The greatest concentration of effective stress is located at the bottom surface of the annular ring. Figure 31(b) shows the effective stress at the final mold displacement resulting in an effective stress of 2.70 MPa at the flow front of the polymer. The total simulation time was established as 5 seconds. The polymer substrate stopped

filling the cavity after 1.20 seconds of molding resulting in a final filling height of 0.27 mm.

Molding temperature was increased to 150°C to study the polymer flow behavior in the second alignment structure. Effective stress evolution is illustrated in Figure 32. Both the flow front of the polymer and the edge of the mold reference points showed similar pressure evolution trends at different effective stress values. Pressure was considerably higher at the edge of the mold. A reduction in pressure is observed around 0.5 mm of mold displacement due to the polymer substrate beating the flow resistance and beginning to flow into the cavity.

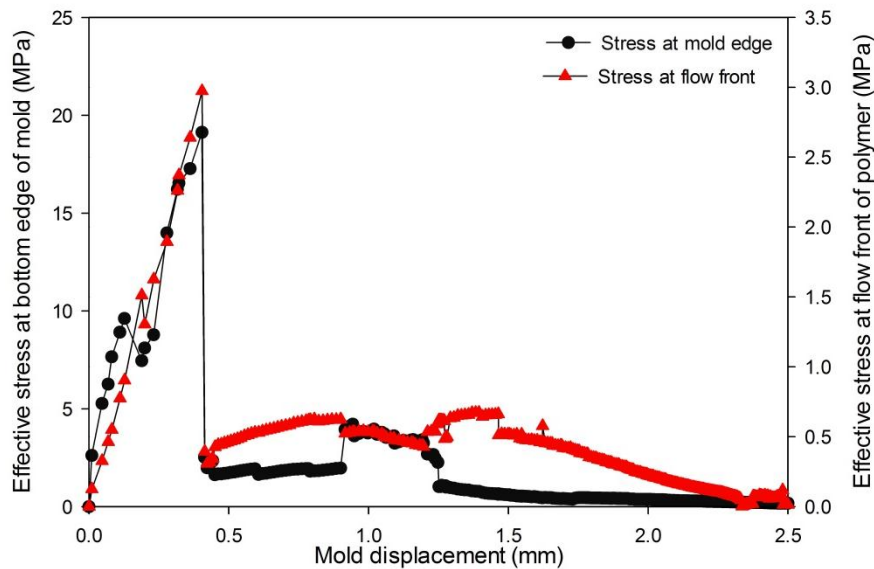


Figure 32. Stress evolution of a molded hemisphere-tipped post with an annular ring at the bottom edge of the mold and the flow front of polymer with a molding temperature of 150°C and a molding force of 300 N.

Effective stress distribution is illustrated in Figure 33. An effective stress of 3.92 MPa was observed at the edge of the mold as presented in Figure 33(a). A filling height

of 0.49 mm was reached at this point. Figure 33(b) shows an increase in pressure caused by the contact generated with the inner wall of the structure.

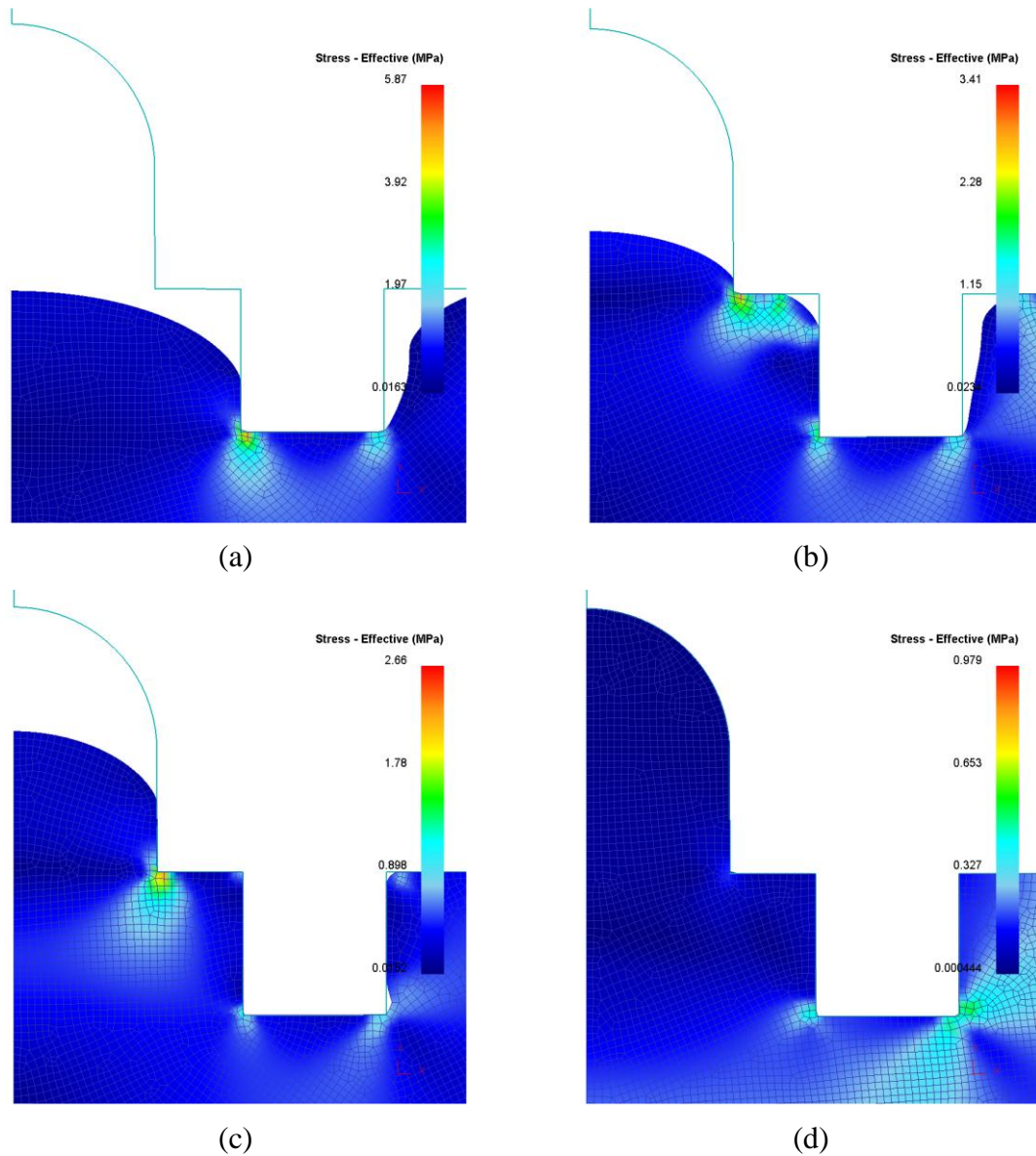


Figure 33. Stress distribution of a molded hemisphere-tipped post in mold filling while the displacement increase from 1.0 mm to 2.5 mm: (a) Mold displacement of 1.0 mm, (b) Mold displacement of 1.5 mm, (c) Mold displacement of 2.0mm, and (d) Mold displacement of 2.5 mm.

Passed 0.86 seconds of embossing a filling height of 0.72 was observed. The cavity was completely filled after 2.68 seconds requiring a total die displacement of 2.48 mm as shown in Figure 33(d).

Effective stress evolution in a cavity filling process at 112.5°C and a molding force of 600 N is shown in Figure 34. The pattern observed under this process parameters is similar to the one found an embossing force of 300 N.

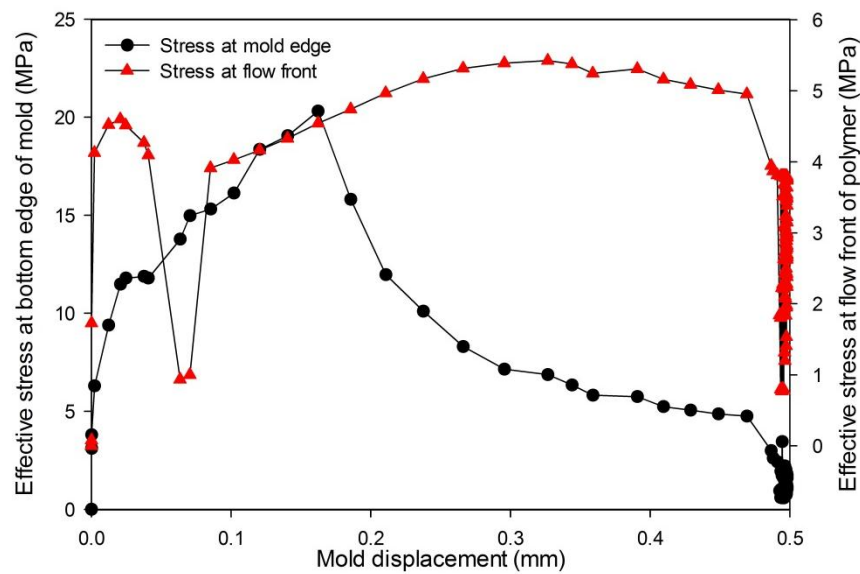


Figure 34. Stress evolution of a molded hemisphere-tipped post with an annular ring at the bottom edge of the mold and the flow front of polymer with a molding temperature of 112.5°C and a molding force of 600 N.

Pressure is higher at 600 N attributable to the increase in the embossing force. It was expected that higher forces would generate higher pressure in the polymer substrate. The flow front of the polymer presents an inflection point after 0.02 mm of displacement caused by annular ring forcing the polymer substrate to flow into the cavity. Effective stress at the edge of the mold increases until the polymer stops flowing into the cavity.

The elevated flow resistance prevents the polymer from filling the cavity. At this point it was noticed that a molding temperature of 112.5°C failed to fill the cavity.

Figure 35 shows the filling heights obtained and the distribution of effective stress. A filling height of 0.26 mm was achieved using a total mold displacement of 0.26 mm. pressure is concentrated at the bottom edges of the annular ring and is spreading downwards as presented in Figure 35(a). After 1.12 seconds the polymer stopped filling the cavity due to the elevated flow resistance. It was noticed a decrease in pressure from this point probably because the polymer is spreading to the sides.

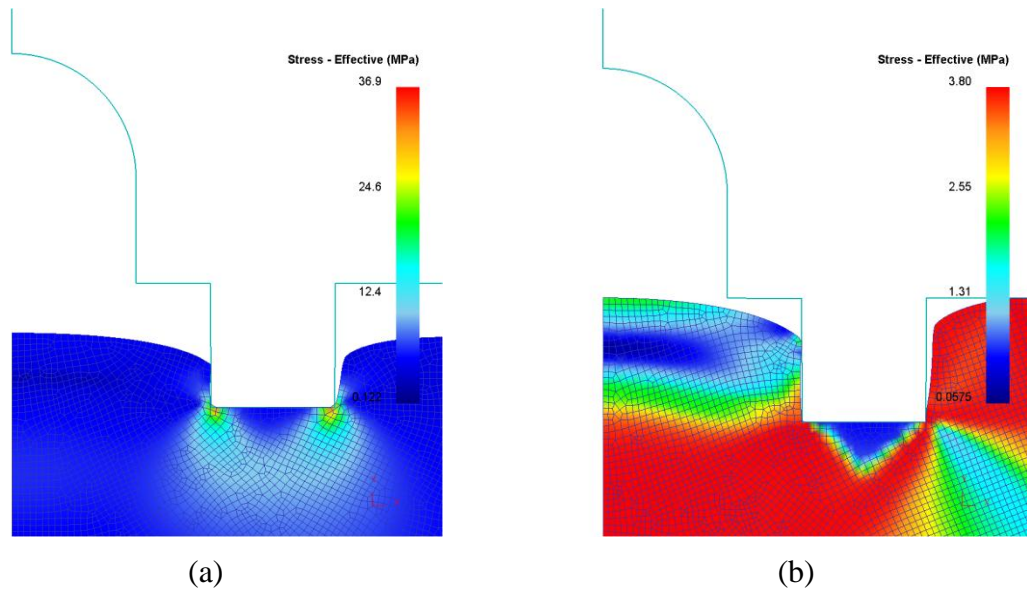


Figure 35. Stress distribution of a molded hemisphere-tipped post in mold filling while the displacement increase from 0.25 mm to 0.50 mm: (a) Mold displacement of 0.25 mm and (b) Mold displacement of 0.50 mm.

Figure 35(b) illustrates the stress distribution at the last moment of the simulation. A mold displacement of 0.5 mm filled 0.27 mm of the hemisphere-tipped hole, resulting in a similar filling height as the one obtained with a molding force of 300 N.

It was noticed that there were not significant differences between the polymer flow behavior at an embossing force of 300 N and the behavior observed at 600 N using a molding temperature of 150°C. The effective stress trend showed various similarities at different pressure rates.

The effective stress distribution at a molding temperature of 150°C and an embossing force of 600 N is illustrated in Figure 4.16. Both the flow front of the polymer and the edge of the mold reference points showed similar trends at different effective stress rates, being higher at the edge of the mold. Pressure decreases drastically after 0.4 mm of displacement when the polymer starts to flow into the structure with reduced flow resistance. The flow front of the polymer presented higher pressure at 1.5 mm of mold displacement caused by the contact generated between these portions of the polymer substrate and the inner walls of the hemisphere-tipped cavity.

A total mold displacement of 1.0 mm produced an effective stress distribution from the edges of the annular ring to the center of this structure, forcing the polymer to flow into the cavity as shown in Figure 36(a). Figure 36(b) illustrates how effective stress is located mostly at the bottom edge of the hemisphere-tipped cavity once the annular ring is completely filled. A filling height of 0.78 mm was observed at this point after 0.72 seconds of embossing.

A mold displacement of 2.5 mm is represented in Figure 36(d). The cavity was filled after 1.65 seconds requiring a total die movement of 2.48 mm.

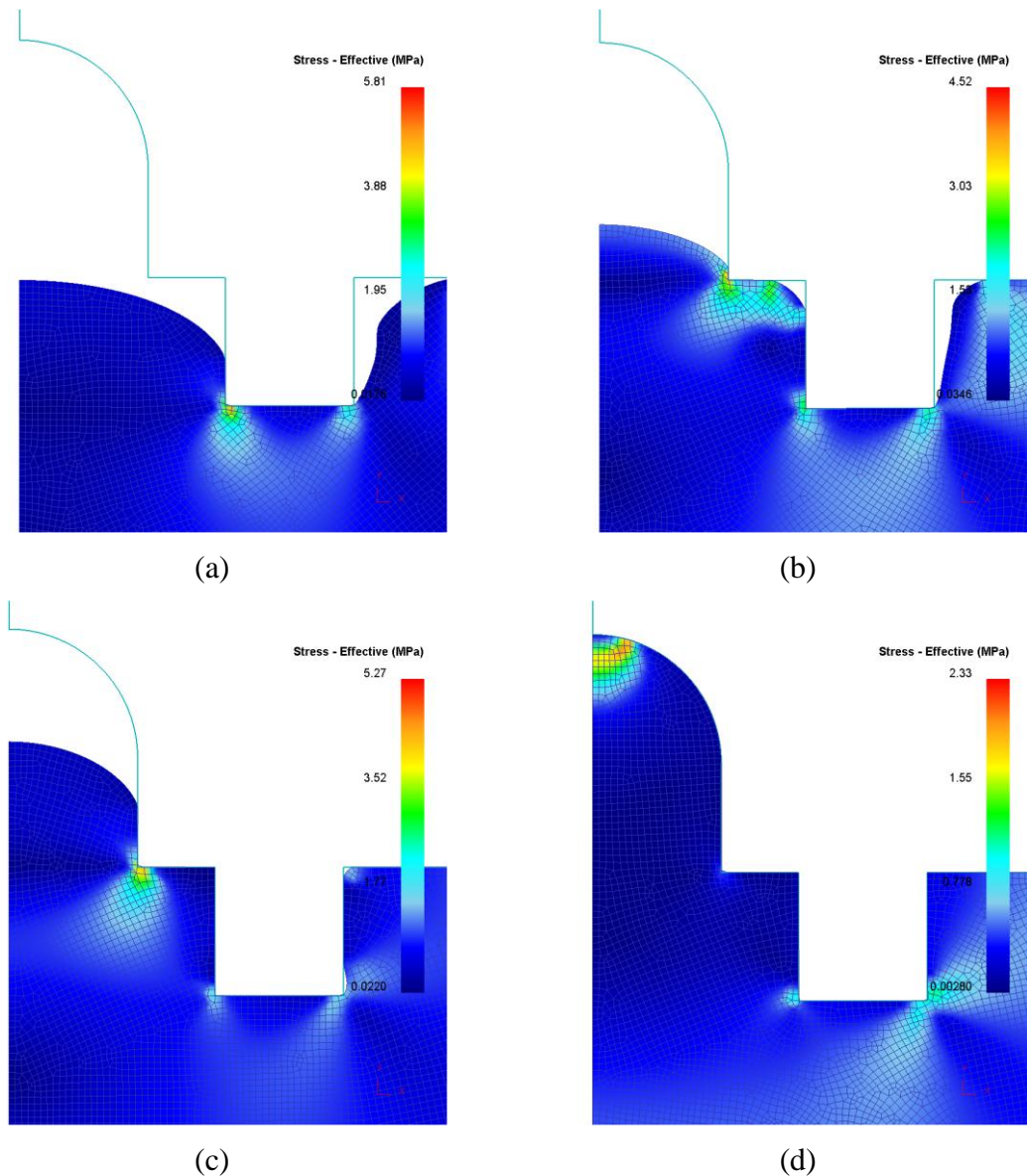


Figure 36. Stress distribution of a molded hemisphere-tipped post in mold filling while the displacement increase from 1.0 mm to 2.5 mm: (a) Mold displacement of 1.0 mm, (b) Mold displacement of 1.5 mm, (c) Mold displacement of 2.0mm, and (d) Mold displacement of 2.5 mm.

The results obtained from the numerical analysis show that the mold displacement required to completely fill the cavity at embossing forces of 300 and 600 N was similar, however, the time required to fill the cavity was reduced almost 1 second using a molding

force of 600 N. it was observed that an increase in the embossing force would affect directly the effective stress on the polymer substrate increasing it as well.

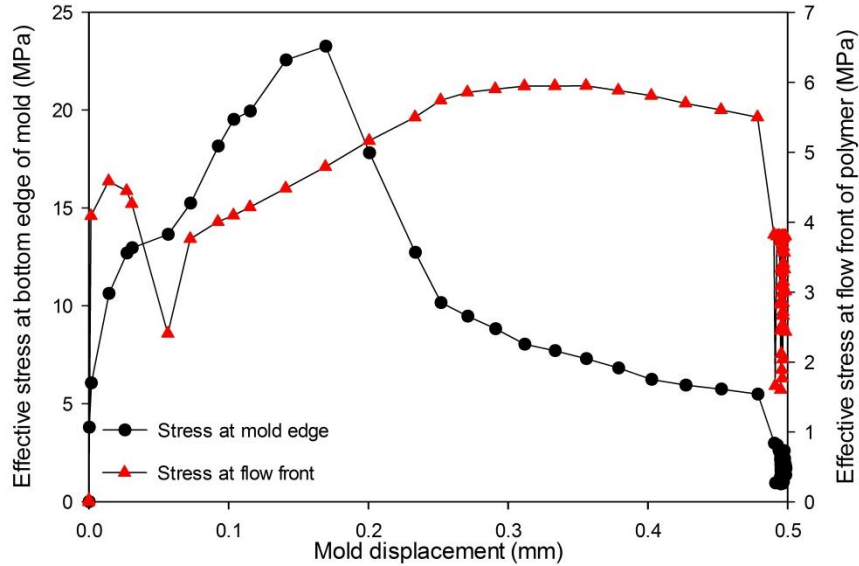


Figure 37. Stress evolution of a molded hemisphere-tipped post with an annular ring at the bottom edge of the mold and the flow front of polymer with a molding temperature of 112.5°C and a molding force of 900 N.

As expected the increase in the embossing force also increased the effective stress on the polymer substrate. Figure 37 illustrates the stress evolution at 112.5°C and a molding force of 900 N. it was noticed that the trend was slightly different compared to other embossing forces included in the numerical analysis. The molding force elevated the effective stress up to 24 MPa at the edge of the mold.

The flow front of the polymer showed reduced effective stress levels compared to the ones obtained at the edges of the mold. This difference in stress at both reference points can be caused by the contact of the polymer with the mold.

The filling heights obtained and the effective stress distribution are represented in Figure 38. After a mold displacement of 0.25 mm the highest stress concentration at these points is caused by the annular ring is the only portion of the top die in contact with the polymer substrate as shown in Figure 38(a). The final step of the molding process resulted in a filling height of 0.29 mm and a mold displacement of 0.5 mm.

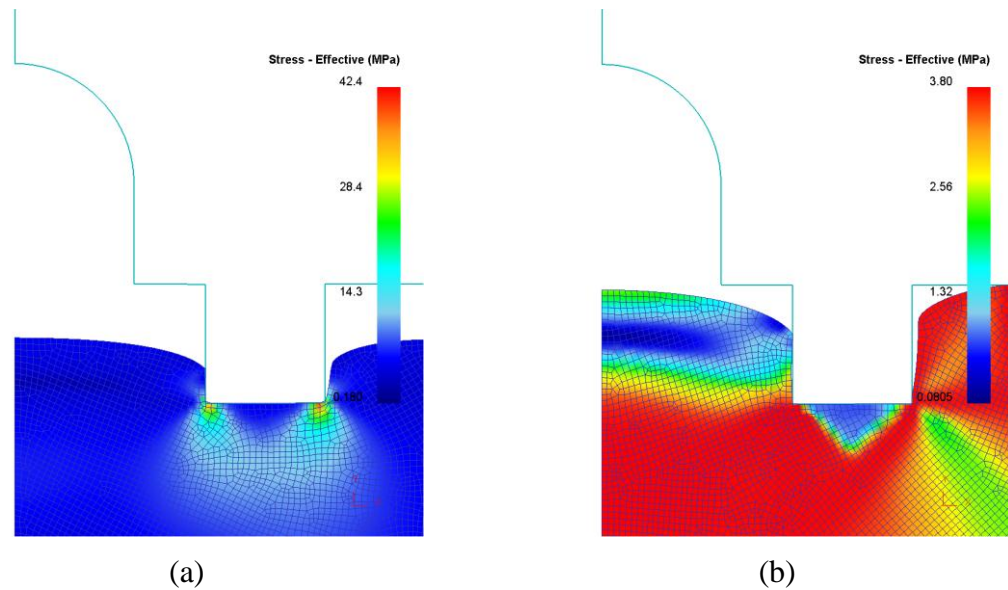


Figure 38. Stress distribution of a molded hemisphere-tipped post in mold filling while the displacement increase from 0.25 mm to 0.50 mm: (a) Mold displacement of 0.25 mm and (b) Mold displacement of 0.50 mm.

Polymer flow behavior at an embossing force of 900 N showed a similar effective stress evolution compared to the results obtained at 300 and 600 N as shown in Figure 39. Effective stress at both reference points is higher at elevated molding forces. The flow front of the polymer and the edge of the mold had similar behavior during the initial 0.4 mm of mold displacement.

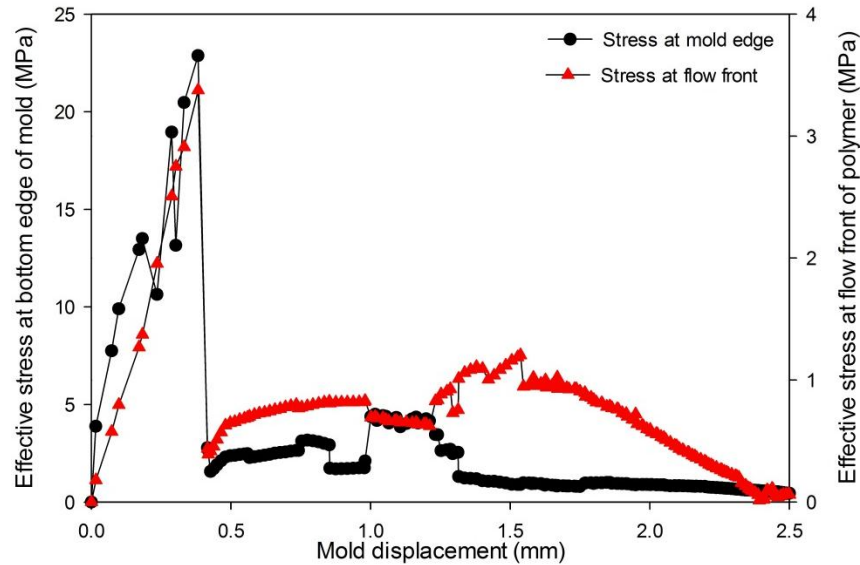


Figure 39. Stress evolution of a molded hemisphere-tipped post with an annular ring at the bottom edge of the mold and the flow front of polymer with a molding temperature of 150°C and a molding force of 900 N.

Effective stress distribution and filling heights are represented in Figure 4.21. Passed 0.37 seconds of embossing a filling height of 0.47 mm was observed with a mold displacement of 1.0 mm as illustrated in figure 40(a). The moment when the polymer reaches the hemisphere-tipped cavity is represented in Figure 40(b).

A mold displacement of 2.0 mm generated a polymer height of 0.98 mm as shown in Figure 40(c). After 0.87 seconds of embossing the effective stress at the flow front of the polymer was 0.6 MPa. Figure 40(d) illustrates the cavity completely filled after 2.5 mm of mold displacement and 1.25 seconds of embossing. A total mold displacement of 2.49 mm was required to fill the cavity after 1.23 seconds of embossing time.

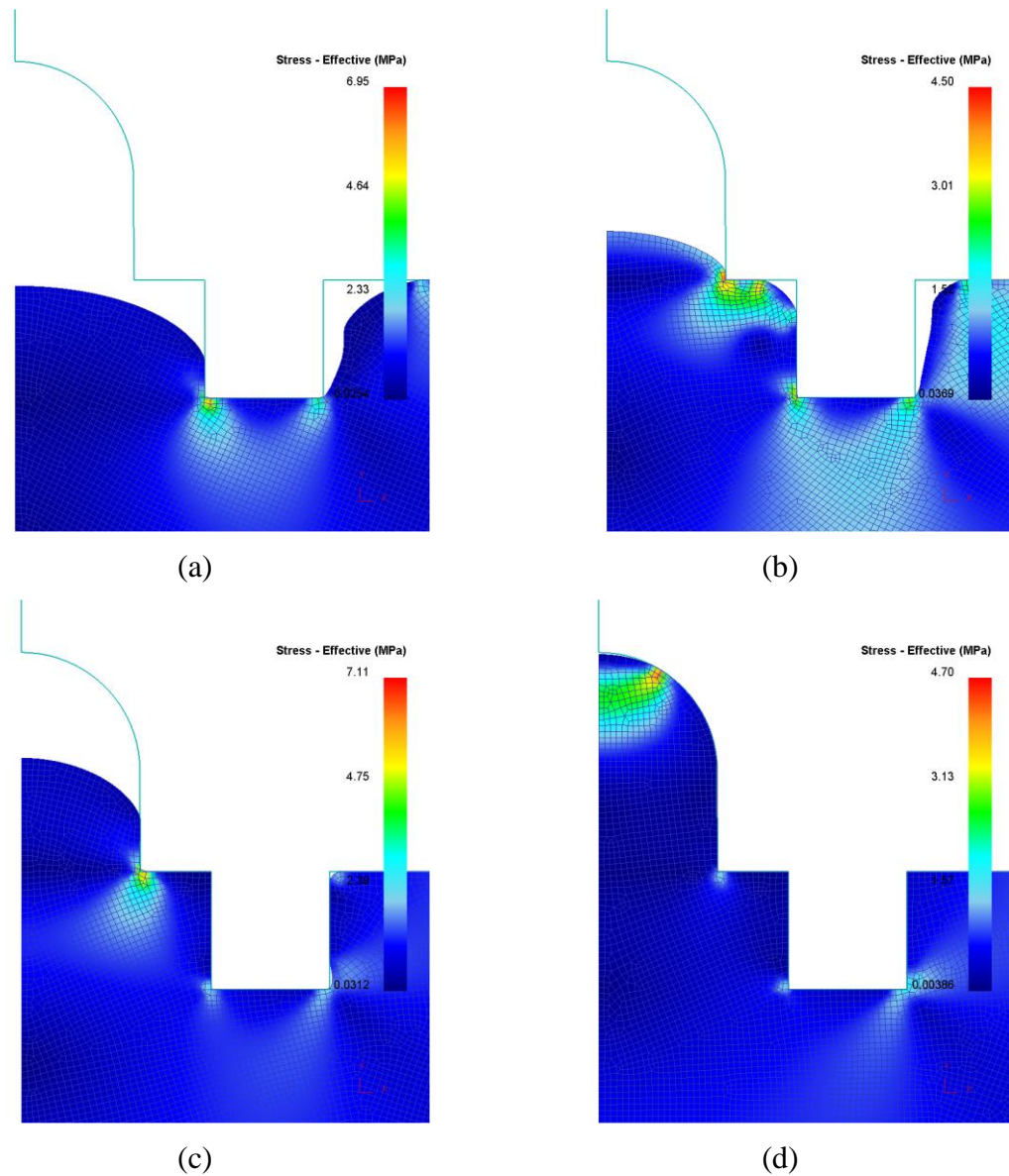


Figure 40. Stress distribution of a molded hemisphere-tipped post in mold filling while the displacement increase from 1.0 mm to 2.5 mm: (a) Mold displacement of 1.0 mm, (b) Mold displacement of 1.5 mm, (c) Mold displacement 2.0 of 2.0mm, and (d) Mold displacement of 2.5 mm.

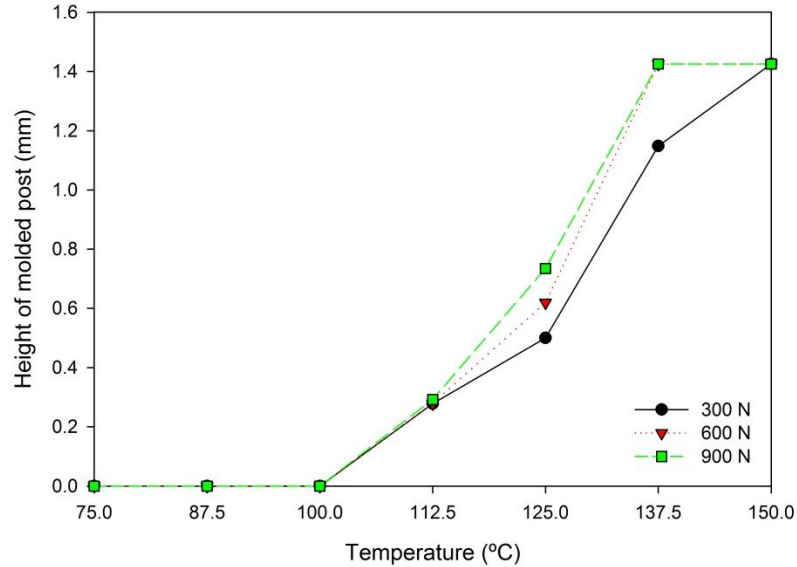


Figure 41. Heights of the molded posts at the molding temperatures of 87.5, 112.5, and 150°C when the displacement increased from 0.5 mm to 2.5 mm.

In Figure 41 the temperatures below T_g failed to generate any deformation at the molding forces included in the numerical analysis. The filling height obtained at 112.5°C was similar in all three forces used. The increase in molding temperature the filling height changed depending on the molding force. It was also noticed that using forces of 600 and 900 N the cavity was completely filled at both 137.5 and 150°C. Effective stress increased also with the increase in the molding force.

4.3 Conclusions

The mold displacement required to fill the cavity was similar under all molding forces studied in this chapter. Nevertheless, the embossing time necessary for the polymer substrate to fill the structure was drastically decreased with the increase in molding force. Effective stress was also elevated as the embossing pressure was increased.

More signs of deformation were observed with the hemisphere-tipped post with an annular ring than with the alignment structure without an annular ring. The extra amount of deformation was caused thanks to the small portion of the mold in contact with the polymer substrate at the initial point of the molding process. A smaller surface in contact means less tension and flow resistance to overcome from the polymer substrate.

It is not possible to say that the hemisphere-tipped post with an annular ring is more efficient in filling the cavities than the hemisphere-tipped post.

CHAPTER 5

CONCLUSIONS

A set of simulations were conducted to analyze the behavior of a polymer substrate in the cavity filling stage of the hot embossing process. The finite element method package chosen to build the simulation model was DEFORM-2D. The numerical model was designed to analyze the effect of the structure design, using two alignment structures: a hemisphere-tipped post and a hemisphere-tipped post with an annular ring, molding temperatures, total die displacement, and molding forces on the polymer flow behavior.

Displacement controlled analysis was performed under the plane geometry model and force controlled simulations were developed using axial-symmetric geometry analysis to reduce calculation time and computer resources. Both simulation methods were built with equal boundary conditions and material properties to validate the obtained results.

The simulation results showed that the polymer was able to completely fill the hemisphere-tipped cavity at molding temperatures of 112.5 and 150°C in both alignment structures: the hemisphere-tipped post and the hemisphere-tipped post with an annular ring, when the total displacement of the top die was fixed at 1.5, 2.0, and 2.5 mm.

The presence of the annular ring helped reducing the stress observed in the polymer substrate. A reduced area in contact with the polymer might be the actual cause of this phenomenon. Simulation results showed that the filling heights observed in both alignment structures was similar. An increased displacement of the polymer substrate was observed in the hemisphere-tipped post with an annular ring suggesting that this added feature was promoting the flow of the polymer into the hemisphere-tipped hole. This effect is caused because the annular ring reduces the flow resistance, preventing the polymer to flow back due to its action as a flow barrier.

Molding forces of 300 and 600 N showed similar results in the filling height and effective stress generated on the polymer substrate. This might be due to the reason that a molding force of 300 N applied a reduced amount of pressure in the polymer substrate. None of the molding forces analyzed generated deformation at all on the polymer at temperatures below T_g . the hemisphere-tipped cavity was completely filled at a process temperature of 150°C.

Partial polymer displacements into the hemisphere-tipped hole were observed at 125 and 137.5°C using a molding force of 300 and 600 N. The hemisphere-tipped hole was completely filled at a molding temperature of 137.5 and 150°C using an embossing force of 900 N. A total die displacement of 0.5 mm was obtained at 112.5°C. After this point the mold stopped penetrating into the polymer substrate due to the reduced pressure applied and that the polymer is not viscous enough to flow easily under these process conditions.

The second alignment structure, a hemisphere-tipped post with an annular ring, showed increasing deformation at 112.5°C than the initial alignment structure analyzed. The filling height at 112.5°C was 0.5 mm, completing almost the total height of the annular ring. Since the polymer was not able to flow and fill the hemisphere-tipped cavity and only completely filled the additional structure it is difficult to analyze the filling heights and the effectiveness of each alignment structure.

In both cases the cavity had a height of 925 μm and it remained empty at the molding temperatures of 112.5°C. In this situation there was no polymer flow observed into the cavities.

The increase in the molding force from 600 to 900 N showed also an increase in the filling height of the polymer substrate and higher values of effective stress were observed in both reference points. Elevated molding forces increased the total process pressure affecting the polymer substrate. It is important to have special attention on the effective stress evolution and distribution on the polymer substrate to avoid failures in the material and reduce quality issues in the terminated product.

The increase in temperature significantly had an effect on the polymer flow behavior during the cavity filling process. The flow resistance of the polymer substrate decreased with the increase of the embossing temperature.

The filling time required by the polymer substrate to completely fill the cavity was also reduced with the increase of the embossing temperature, demonstrating the in fact the fluidic resistance of the polymer substrate decreased.

The proper molding temperature, mold displacement, and molding forces can be chosen by analyzing the polymer flow behavior obtained in the simulations.

REFERENCES

- Chen, P.-C., You, B., Park, D., Park, S., Nikitopoulos, D., Soper, S., et al. (2007).
Replication of reliable assembly features for polymer modular microfluidic
systems. *Proceedings of the ASME IMECE 2007* (pp. 1-6). Seattle: ASME.
- G'Sell, C., & Souahi, A. (1997). Influence of crosslinking on the plastic behavior of
amorphous polymers at large strains. *Journal of Materials and Technology*, 223-
227.
- He, Y., Fu, J.-Z., & Chen, Z.-C. (2007). Research on optimization of the hot embossing
process. *Journal of Micromechanics and Microengineering*, 2420-2425.
- Heckeke, M., & Schomburg, W. (2004). Review on micro molding of thermoplastic
polymers. *Journal of Micromechanics and Microengineering*, R1-R14.
- Heyderman, L. J., Schiff, H., David, C., Gobrecht, J., & Schweizer, T. (2000). Flow
behavior of thin polymer films used for hot embossing lithography.
Microelectronic Engineering, 229-245.
- Hosford, W., & Caddell, R. (2011). *Metal forming mechanics and metallurgy*.
Cambridge: Cambridge University Press.

- Jin, P., Gao, Y., & Liu, T. (2009). Simulation of filling characteristics during hot embossing of polymer microstructures. *Fifth International Symposium on Instrumentation Science and Technology*. Harbin: SPIE.
- Jin, P., Gao, Y., Liu, T., Tan, J., Wang, Z., & Zhou, H. (2009). Simulation and experimental study on recovery of polymer during hot embossing. *Japanese Journal of Applied Physics*.
- Juang, Y.-J., Lee, J., & Koelling, K. (2002). Hot embossing in microfabrication. Part I: experimental. *Polymer Engineering and Science*, 539-550.
- Juang, Y.-J., Lee, J., & Koelling, K. (2002). Hot embossing in microfabrication. Part II: rheological characterization and process analysis. *Polymer Engineering and Science*, 551-566.
- Kiew, C., Lin, W.-J., Teo, T., Tan, J., & Lin, W. (2009). Finite element analysis of PMMA pattern formation during hot embossing process. *IEEE/ASME International Conference and Advanced Intelligent Mechatronics* (pp. 314-319). Singapore: IEEE.
- Lin, C. R., Chen, R. H., & Hung, C. (2002). The characterisation and finite-element analysis of a polymer under hot embossing. *Advanced Manufacturing Technology*, 230-235.
- Lin, C. R., Chen, R. H., & Hung, C. (2003). Preventing non-uniform shrinkage in open-die hot embossing of PMMA microstructures. *Materials Processing Technology*, 173-178.

- Liu, C., Li, J. M., Liu, J. S., & Wang, L. D. (2010). Deformation behavior of solid polymer during hot embossing process. *Microelectronic Engineering*, 200-207.
- Lou, Y., Xu, M., Wang, X., & Liu, C. (2006). Finite element analysis of PMMA microfluidic chip based on hot embossing technique. *Journal of Physics*, 1102-1106.
- Lu, C., Juang, Y.-J., & Lee, J. (2005). Analysis of laser/IR-assisted microembossing. *Polymer Engineering and Science*, 661-668.
- Luche, J., Rogaume, T., Richard, F., & Guillaume, E. (2011). Characterization of thermal properties and analysis of combustion behavior of PMMA in a cone calorimeter. *Fire Safety Journal*, 451-461.
- Scientific Forming Technologies Corporation. (2010). *DEFORM Design Environment for Forming*. Columbus: SFTC.
- Worgull, M. (2009). *Hot embossing theory and technology of microreplication*. Burlington: William Andrew.
- Worgull, M., & Hecke, M. (2004). New aspects of simulation in hot embossing. *Microsystems Technology*, 432-437.
- Worgull, M., Hetu, J. F., & Kabanemi, K. K. (2006). Modeling and optimization of the hot embossing process for micro- and nanocomponent fabrication. *Microsystems Technology*, 947-952.
- Wu, C.-H., Hung, C.-H., & Hu, Y.-Z. (2009). Parametric study of hot embossing on micro-holes. *Advanced Materials Research*, 251-254.

- Wu, H., Ma, G., & Xia, Y. (2004). Experimental study of tensile properties of PMMA at intermediate strain rate. *Materials Letters*, 3681-3685.
- Yao, D., & Virupaksha, V. (2005). Study on squeezing flow during nonisothermal embossing of polymer microstructures. *Polymer Engineering and Science*, 652-660.
- You, B., Chen, P.-C., Park, D., Park, S., Nikitopoulos, D., Soper, S., et al. (2009). Passive micro-assembly of modular, hot embossed, polymer microfluidic devices using exact constraint design. *Journal of Mechanics and Microengineering*, 1-11.
- Young, W.-B. (2005). Analysis of the nanoimprint lithography with a viscous model. *Microelectronic Engineering*, 405-411.
- Zhang, T., He, Y., & Fu, J. (2011). Simulation research on stress of polymeric patterns during micro hot embossing. *Applied Mechanincs and Materials*, 339-345.

VITA

Juan A. Gomez was born in Bogota, Colombia, on June 26, 1984. He received the degree of Bachelor of Science in Industrial Engineering at Universidad de La Sabana, Colombia in 2009. During the following years he worked in the industry as a Research and Development assistant and a Supply Chain supervisor in two major companies located in Quito, Ecuador. Juan entered the College of Science and Engineering at Texas State University-San Marcos in August 2009, focusing his research interests in polymer micromanufacturing. After receiving his Master of Science degree Juan is planning to continue his research in the Doctoral program offered at Texas State.

Permanent address: 1518 Old Ranch Road 12 APT 1402

San Marcos, TX 78666

This thesis was typed by Juan Andres Gomez.